Rho GTPase family members in establishment of polarity in *C. elegans* embryos

DISSERTATION

zur Erlangung des akademischen Grades

Doctor rerum naturalium

(Dr. rer. nat)

vorgelegt

der Fakultät Mathematik und Naturwissenschaften

der Technischen Universität Dresden

von

STEPHANIE SCHONEGG

geboren am 28. Juni 1975, Basel (Schweiz)

Gutachter: Prof. Dr. Anthony A. Hyman
                                    Prof. Dr. Juergen A. Knoblich
                                    Dr. Carl-Philipp Heisenberg

Eingereicht am   5. September 2005

Tag der Verteidigung   29. November 2005

TABLE OF CONTENTS

SUMMARY

Cell polarity is required for asymmetric division, a mechanism to generate cell diversity by distributing fate determinants unequally to daughter cells. The establishment of polarity requires the evolutionarily conserved partitioning-defective (PAR) proteins as well as the actin cytoskeleton. In *Caenorhabditis elegans* one-cell embryos, the PAR proteins are segregated into an anterior (PAR-3, PAR-6) and a posterior (PAR-1, PAR-2) cortical domain. The formation of PAR polarity correlates with anterior-posterior differences in the contractile activity of the cortex, known as "contractile polarity". It is thought that regulation of contractile polarity controls the establishment of PAR polarity, but detailed evidence to support this idea is lacking. To investigate how modulation of the acto-myosin cytoskeleton affects polarity establishment, the acto-myosin cytoskeleton was perturbed by RNA-mediated interference (RNAi) of two Rho GTPases, CDC-42 and RHO-1. To examine how Rho GTPases are implemented in actin remodeling, it is important to analyze how their activity is controlled and how different activities affect polarity formation. The role of two putative Rho GTPase regulators, the Rho GTPase exchange factor (GEF) ECT-2 and the Rho GTPase activating protein (GAP) K09H11.3 were analyzed with respect to polarity formation. The formation of polarity was analyzed by using GFP-labeled proteins, and several different tracking methods were used to investigate the establishment of contractile and PAR polarity in more detail.

This study demonstrates that both RHO-1 and CDC-42 are involved in polarity establishment in *C. elegans* embryos. But importantly, both act by different mechanisms. RHO-1 organizes the acto-myosin cytoskeleton into a contractile network, and therefore is essential for the formation of contractile polarity. The organization of the acto-myosin cytoskeleton is critical to ensure proper PAR protein distribution. Furthermore, a balance of RHO-1 activity by the GEF ECT-2 and the GAP K09H11.3 appears to be important for cortical contractility, for PAR protein domain size and for mutual exclusion of the PAR proteins. Although CDC-42 was shown to be a universal regulator of the actin cytoskeleton, CDC-42 acts downstream of contractile polarity. CDC-42 is required for linking PAR-6 to the cortex. In the absence of RHO-1 and ECT-2, PAR-6 and CDC-42 are not localized to the anterior cortex. This suggests that RHO-1, by organizing the acto-myosin cytoskeleton into a contractile network, regulates the segregation of CDC-42 to the anterior cortex, and concomitantly PAR-6 localization. This study shows that the distribution of PAR is related to cortical activity and supports the model that the actin cytoskeleton plays an important role in polarity establishment.

1. INTRODUCTION

The establishment of cell polarity is reflected by the asymmetric distribution of proteins within the cell, often coupled with accompany of cellular asymmetry. Cell polarization is essential for all cellular differentiation and thus occurs throughout the Metazoa. Examples of cell polarity include axon outgrowth in neurons, pseudopod extension by migrating cells, and fate specification during stem cell divisions. Consistent with the many contexts of cellular polarization, polarity establishment has been studied in many systems. Much of our understanding of cell polarity comes from studies of apical-basolateral axis establishment of epithelial cells, formation of the anterior-posterior axis of *Caenorhabditis elegans (C. elegans)* and *Drosophila melanogaster* embryos, cell fate determination in the *Drosophila melanogaster* nervous system, leading-edge polarization in migrating cells, and bud-site selection in the yeast *Saccharomyces cerevisiae (S. cerevisiae)* (Macara, 2004; Ohno, 2001).

Despite the different biological contexts, many features of polarity are quite general and can be conceptualized as a hierarchical sequence of several steps (Drubin and Nelson, 1996). To establish polarity, the axis of symmetry must be broken as an axis of division is specified. The symmetry-breaking event can occur spontaneously, or it can be triggered by an external cue, such as soluble molecules (growth factors, cytokines and hormones) that bind to surface receptors, adhesive interactions (contact of another cell and to extracellular matrix), mechanical stress (tension, fluid shear stress), or fertilization (Schwarz et al. 2004). In response to the symmetry-breaking event, cell polarization takes place. The asymmetry is propagated and stabilized through the re-distribution of "polarity proteins" into different regions of the cell. These polarized cellular domains then direct the accumulation of fate determinants, the molecules that will produce the functional aspects of the cellular asymmetry (for example, lamellipodia protrusion or differentiation into muscle cell).

Polarized cells may achieve their function as a single cell, as in neurons, or the asymmetric function may require that they divide asymmetrically, as in stem cells. The divisions of such polarized cells must ensure the proper segregation of fate determinants to daughter cells. During mitosis, the spindle is oriented along the polarity axis, and after cytokinesis both cell differ in their content of cell fate determinants.

Conserved mechanisms regulate polarity. The predominant molecules are PAR proteins, the actin cytoskeleton, and microtubules. Correlating reports from different systems showed that PAR proteins become asymmetrically distributed during polarization and that they function in transmitting the initial polarity cue to downstream events such as spindle positioning and distribution of cell fate determinants (Cowan and Hyman, 2004a; Macara, 2004; Ohno, 2001). The actin cytoskeleton was identified as an important target of the polarizing cue. Initiation of polarity induces dramatic cytoskeletal rearrangements leading to a morphological polarization and polarized distribution of downstream molecules including PAR proteins. Microtubules play a critical role in directed transport of proteins and vesicles required for cell polarization (Fukata et al., 2003). The Rho GTPases family proteins are important for mediating the polarizing signal to the actin cytoskeleton as well as to microtubules (Etienne-Manneville and Hall, 2002; Jaffe and Hall, 2005).

1.1 The *C. elegans* embryo as a model organism to study cell polarity

The *C. elegans* is a free-living soil nematode, about 1 mm in length. The worms develop from eggs to fertile adults in about three days. In the laboratory, the worms are kept on agarose plates and fed with *Escherichia coli*. Their short reproductive life cycle and simple maintenance in the laboratory make *C. elegans* a powerful model organism (Wood, 1988). The worms have two sexes, hermaphrodites and males, consisting of a fixed number of cells, 959 or 1031, respectively. Hermaphrodites reproduce by either self-fertilization or mating and lay about 300 eggs during the reproductive life cycle. Males spontaneously arise by X-chromosome nondisjunction at meiosis at a low frequency. Most of the embryonic development occurs outside of the uterus. Production of a chitinous eggshell protects the embryo from environmental influences.

The anatomy of the nematode is quite simple, and the animals are transparent throughout the life cycle, which allows the study of the development at a cellular level in living animals using light microscopy. The embryos are relatively large (about 50 μm), and therefore, the embryonic development can be easily followed by time-lapse differential interference contrast (DIC) microscopy. The morphological changes in the embryo are simple to follow: the nuclei and the centrosomes appear as cytoplasmic clearings within the mass of yolk granules in the embryo, which helps to determine the cell cycle stage. Changes in cortical activity, or ruffling, are easily observed and provide a marker of

cortical polarity. Furthermore, tracking the movement of yolk granules allows an analysis of polarized cytoplasmic flows, a manifestation of polarity establishment. Time-lapse microscopy of GFP-labeled proteins allows the analysis of the role of proteins of interest in different processes in the embryo. The embryonic development takes about 45 minutes from meiosis to cytokinesis. The first mitotic division in *C. elegans* embryos is asymmetric. A genetic screen for maternal-effect mutations affecting asymmetric cell division identified the PAR (partitioning-defective) proteins as important molecules for cell polarization (Kemphues et al., 1988). The following twenty years of research identified many other proteins involved in cell polarity and the *C. elegans* early embryo became a well-established system for studying cell polarity.

The completion of the sequencing of the *C. elegans* genome which contains about 19'000 predicted genes (http://www.wormbase.org), permits the identification of genes potentially involved in certain processes. Furthermore, the discovery of the technique of RNA-mediated interference (RNAi) helps to dissect cellular processes (Fire et al., 1998). RNAi allows depletion of a given gene by introducing the corresponding double-stranded RNA. Using RNAi a series of large-scale functional genomics analysis were performed, which identified the genes for cell division (Fraser et al., 2000; Gonczy et al., 2000; Sonnichsen et al., 2005; Zipperlen et al., 2001) and are very useful source of information for further detailed studies concerning the mechanisms of cell polarity.

1.2 The role of PAR proteins in cell polarity

The PAR (partitioning-defective) proteins were discovered in *C. elegans* through a genetic screen for maternal-effect mutations affecting asymmetric cell division (Kemphues et al., 1988). Mutations in PAR proteins results in mislocalization of other cell polarity proteins, leading to the disruption of cell polarity. PAR proteins are conserved throughout the Metazoa and have been demonstrated to play an important role in anterior-posterior polarity in *C. elegans* and *Drosophila* embryos, apical-basolateral polarization in epithelial cells, neuroblast polarity, oriented cell migration, planar polarity, and neuronal-axon specification (Cowan and Hyman, 2004a; Knoblich, 2001; Macara, 2004; Ohno, 2001; Schneider and Bowerman, 2003; Wang and Chia, 2005). In general, the PAR proteins can be viewed as polarity-transducing molecules: they respond to the initial polarization cue and establish stable domains that can be recognized by fate determinants.

1.2.1 The PAR protein family

PAR proteins display functional similarities but are divergent in sequence (Figure 1A). PAR-1 and PAR-4 are protein kinases (Guo and Kemphues, 1995; Watts et al., 2000). PAR-3 and PAR-6 contain PDZ domains (Etemad-Moghadam et al., 1995; Hung and Kemphues, 1999) and PAR-5 is a 14-3-3 protein (Morton et al., 2002). PAR-2 contains a RING finger and is the only PAR protein that does not appear to be conserved (Levitan et al., 1994). aPKC-3, the seventh member of this group based on its interaction with PAR-3 and PAR-6 (see below), was later identified by homology to an atypical protein kinase C (Tabuse et al., 1998) (Figure 1B). In vertebrates, several PAR proteins exist as multiple isoforms: four each for PAR-1 and PAR-6 and two for PAR-3 (Macara, 2004).

1.2.2 The PAR-3/PAR-6/aPKC complex displays evolutionary conserved function

The PAR proteins localize to specific domains in the cell. PAR-3 and PAR-6 form an evolutionary conserved complex with aPKC-3 (Etemad-Moghadam et al., 1995; Tabuse et al., 1998; Watts et al., 1996), which has emerged as a central player in regulating cell polarity. In all systems in which it has been studied, the PAR-3/PAR-6/aPKC complex becomes asymmetrically localized, and restricts other polarity proteins to the opposite side of the cell. The complex has also been implicated in spindle positioning (Ohno, 2001). For instance, in *C. elegans* embryos, the PAR-3/PAR-6/aPKC complex is required

9

to restrict PAR-1 and PAR-2 to the posterior cortex in the one-cell embryo. Depletion of a member of this complex results in uniform localization of PAR-1 and PAR-2 (Cuenca et al., 2003; Etemad-Moghadam et al., 1995; Hung and Kemphues, 1999; Tabuse et al., 1998; Watts et al., 1996). The asymmetric localization of the mitotic spindle fails, resulting in two daughter cells equal in size (Cheng et al., 1995; Kemphues et al., 1988). Likewise, in *Drosophila* neuroblasts, the PAR-3-PAR-6-aPKC complex localizes apically. Mutations in PAR proteins affect the distribution of basal components and cause randomized orientation of the spindle (Petronczki and Knoblich, 2001; Schober et al., 1999; Wodarz et al., 1999). In mammalian epithelial cells, the PAR-3-PAR-6-aPKC complex localizes to the apical zone of tight junctions (Izumi et al., 1998). Tight junctions act as fences in epithelia by preventing the free mixing of proteins and lipids of apical and basolateral membrane compartments. Overexpression studies of aPKC mutant lacking kinase activity in MDKC cells caused mislocalization of tight junctions proteins and thus apical-basolateral polarity (Joberty et al., 2000).

A

PAR-1, PAR-2, PAR-3, PAR-4, PAR-5, PAR-6, aPKC domain structures
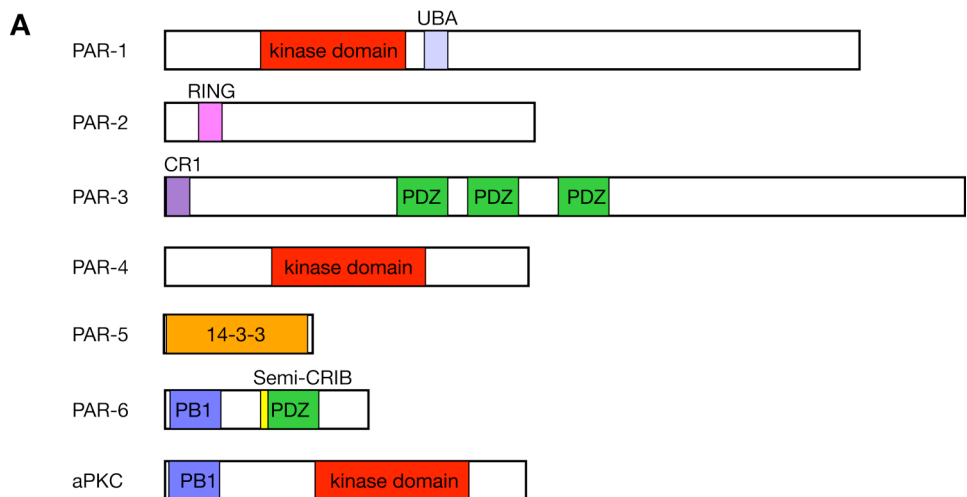
B

C. elegans	Drosophila	Mammals
PAR-1	Par-1	MARK, PAR-1, CTAK, KP78., EMK
PAR-2	not identified	not identified
PAR-3	Bazooka	PAR3, ASIP
PAR-4	Lkb1	LKB1/STK11
PAR-5	14-3-3	14-3-3
PAR-6	Par-6	PAR6A-PAR6D
aPKC-3	aPkc	PKC
CDC-42	Cdc42	CDC42
RHO-1	Rho1, RhoA	RHOA
ECT-2	Pebble	ECT-2
K09H11.3	not identified	not identified

Figure 1. PAR proteins

(A) Domain structure of PAR proteins. UBA (ubiquitin associated domain) is found in proteins connected to ubiquitin pathways. RING domains are often associated with E3 ubiquitin-protein ligase activity. CR1 (conserved region 1) is required for PAR-3 oligomerization. PDZ (PDS-95, Discs large, Zona occludens-1) binds other PDZ domains and carboxy-terminal motifs such as Thr/Ser-X-/Val (X is any amino acid). 14-3-3 binds to phosphoserines and phosphothreonines. PB1 (phagocyte oxidase/Bem1) binds other PB1 domains. CRIB (Cdc-42/Rac-interactive binding) binds Rac/Cdc-42 family members in the GTP-bound state. **(B)** Polarity proteins and Rho GTPase family members in other systems.

1.3 The role and regulation of the actin cytoskeleton during cell polarization

1.3.1 The actin cytoskeleton displays structural and mechanical properties

The actin cytoskeleton provides the structural basis for cell morphogenesis and cell polarity development (Bretscher, 1991). It is a highly dynamic meshwork that provides mechanical support (Pollard and Borisy, 2003) and facilitates movement of molecules and organelles within the cell. Actin is one of the most abundant proteins in cells and exists either as globular monomer (G-actin) or as filament (F-actin). The actin filament is a polar structure and is formed by head to tail polymerization of G-actin. Actin filament formation starts with the formation of actin dimer, a step, which is extremely unfavorable (Pollard, 1986). The addition of a third actin monomer to form a trimer makes the complex more stable, and the trimer formation allows subsequent binding of additional actin monomers leading to an elongating filament. The regulating of the nucleation step is critical for controlling the initiation of actin polymerization and involves several regulators including the Arp2/3 complex and profilin (see below). Each monomer binds an ATP molecule that is hydrolyzed following polymerization. This creates polarity in the actin filament. The "new" (barbed) end contains ATP-bound monomers, the neighboring part of the filament is composed of monomers containing ADP and unreleased-phosphate (ADP-Pi) and the "old" end contains ADP-bound monomers from which the phosphate has been released (May, 2001). The names barbed and pointed correspond to the arrowhead appearance of myosin heads bound to actin filaments. Actin monomers assemble much more rapid at the barbed end, compared to the pointed end. Many protein bind to actin filaments and influence its dynamic or state. Capping proteins (e.g. gelsoline) bind to the barbed end and prevent further elongation. Severing proteins (e.g. ADF/cofilin) cause fragmentation of actin filaments. Crosslinking proteins (e.g. α-actinin, fimbrin) and bundling proteins (e.g villin) organize actin filaments into parallel bundles or into branched networks, depending on the cellular context (Pollard et al., 2000; Revenu et al., 2004).

1.3.2 The role of actin in cell polarity

Extracellular or endogenous signals induce reorganization of the actin cytoskeleton, which leads to polarized cell morphology, and polarized distribution of downstream molecules. Bundling of parallel actin filaments into cables stabilized by tropomyosins, serve as tracks for myosin-V-mediated transport of vesicles, an essential process for cell polarization (Bretscher, 2003). The assembly of actin filaments and myosin II into

contractile filaments provides the mechanical force for cortical contraction and for cytokinesis. The generation of tension and contractile forces are required for polarized cell shape and cell migration (Etienne-Manneville and Hall, 2002; Glotzer, 2005).

1.3.3 Rho GTPases are regulators of the actin cytoskeleton

Cell polarization depends on communicating a symmetry-breaking event to induce a reorganization of the actin cytoskeleton, leading to polarized cellular domains and an asymmetric distribution of cytoskeletal function. The Rho GTPases play important roles in signaling to the downstream cellular machinery that controls actin cytoskeleton organization. Rho family GTPases belong to a subfamily of small (~21 kDa) GTP-binding proteins that are related to Ras. They are evolutionarily conserved at both structural and functional levels (Wherlock and Mellor, 2002) and were identified as regulators of the actin cytoskeleton by using constitutively activated mutants of the prototype members RhoA, Cdc42 and Rac1. Rho was shown to promote the assembly of focal adhesion and the assembly of contractile actin and myosin filaments into stress fibers (Ridley and Hall, 1992), whereas activated Rac created actin-rich surface protrusions (lamellipodia) (Ridley et al., 1992). Cdc42 promoted actin-rich membrane extensions, the filopodia (Kozma et al., 1995; Pruyne and Bretscher, 2000). Further analysis revealed that the three GTPases use different signaling pathways to assemble the distinct actin structures (Etienne-Manneville and Hall, 2002). In addition to signal pathways linked to the actin cytoskeleton, Rho GTPases participate in the regulation of gene transcription, G1 cell cycle progression, microtubule dynamics and vesicle transport (Jaffe and Hall, 2005).

1.3.4 Members of the Rho GTPase family

A large number of genes encoding for Rho GTPases have been identified, but their number varies between organisms. The mammalian genome contains 23 Rho GTPases, the yeast *S. cerevisiae* genome encodes six Rho GTPases and seven GTPases were identified in *Drosophila melanogaster* and in *C. elegans,* respectively (Caruso et al., 2005; Wherlock and Mellor, 2002). The Rho GTPases can be divided into 8 classes: RhoA-related proteins (RhoA, RhoB and RhoC), Cdc42-related proteins (Cdc42, TC10, TCL, Wrch-1, Chp), Rac1-related proteins (Rac1, Rac2, Rac3 and RhoG), Rnd proteins (Rnd1, Rnd2, Rnd3), RhoBTB proteins (RhoBTB1, -2, -3), RhoD proteins (RhoD and Rif), RhoH and Miro proteins (Miro1 and Miro2) (Aspenstrom et al., 2004).

Similarly to RhoA, Cdc42 and Rac1, the constitutively activated forms of Rnd and RhoD proteins induce actin reorganization in the cell. Rnd proteins were shown to induce the formation of microvilli, whereas the RhoD proteins promoted the formation of long and flexible filopodia. In contrast, RhoBTB proteins, RhoH as well as the Miro proteins do not induce actin remodeling (Aspenstrom et al., 2004).

1.3.5 The *C. elegans* Rho GTPases

The *C. elegans* Rho GTPases can be classified into three sequence-related groups according to their mammalian orthologs (Figure 2B): One RhoA-related protein (RHO-1), two Cdc42-related proteins (CDC-42, CRP-1) and three Rac1-related proteins (CED-10, RAC-2, MIG-2). CHW-1, the seventh member is a Wrch-like protein, has not been characterized yet (Caruso et al., 2005).

RHO-1 and CDC-42 appear to be the only Rho GTPases that play essential roles in the one-cell embryo. RHO-1 is required for cytokinesis (Jantsch-Plunger et al., 2000), whereas CDC-42 is implicated in polarity formation (Gotta et al., 2001; Gotta and Ahringer, 2001; Kay and Hunter, 2001). The Rac1-related proteins are required at later developmental stages. CED-10, RAC-2 and MIG-2 are involved in axon guidance and cell corpse phagocytosis. CED-10, MIG-2 and RHO-1 also participate in cell migration (Lundquist et al., 2001; Reddien and Horvitz, 2000; Spencer et al., 2001; Wu et al., 2002; Zipkin et al., 1997), whereas CRP-1 is involved in apical membrane trafficking in epithelial cells (Jenna et al., 2005).

1.3.6 Regulation of Rho GTPases

Rho GTPases act as molecular switches cycling between an active GTP-bound state and an inactive GDP-bound state (Figure 2A). Three classes of regulatory proteins control the GTPase activity. Guanine nucleotide exchange factors (GEFs) activate GTPases by catalyzing the exchange of GDP for GTP (Schmidt and Hall, 2002), whereas GTPase activating proteins (GAPs) inactivate GTPases by stimulating the intrinsic GTPase activity (Bernards, 2003). Guanine nucleotide dissociation inhibitors (GDIs) are required to block spontaneous activation (Olofsson, 1999). Moreover, the Rho GTPases can be regulated by phosphorylation or ubiquitination, however, to what extent this modifications play a role is not yet clear (Bryan et al., 2005; Lang et al., 1996; Wang et al., 2003). Given that Rho GTPases are implicated in a large number of biological processes, each GAP and GEF may selectively, regulate spatially and temporally a specific Rho GTPase pathway.

Another level of regulation is the control of the activity of GAPs and GEFs themselves also in a spatial and temporal manner, which increases the complexity of Rho GTPases signaling pathways.

A

B
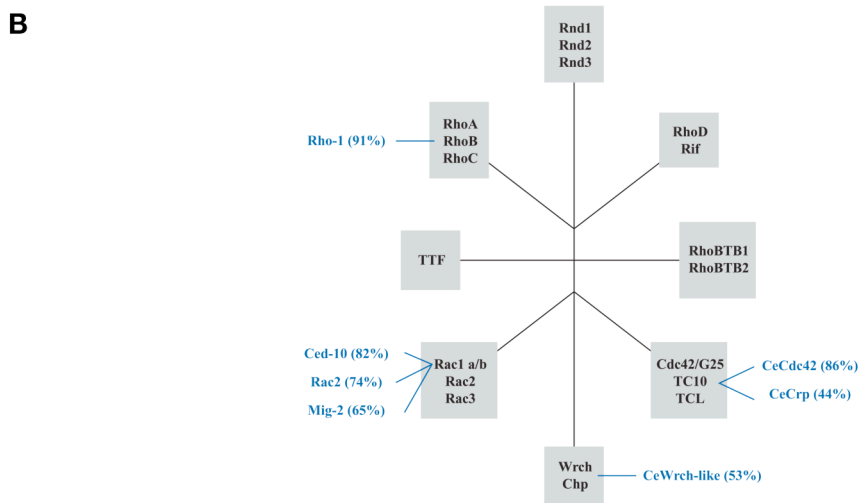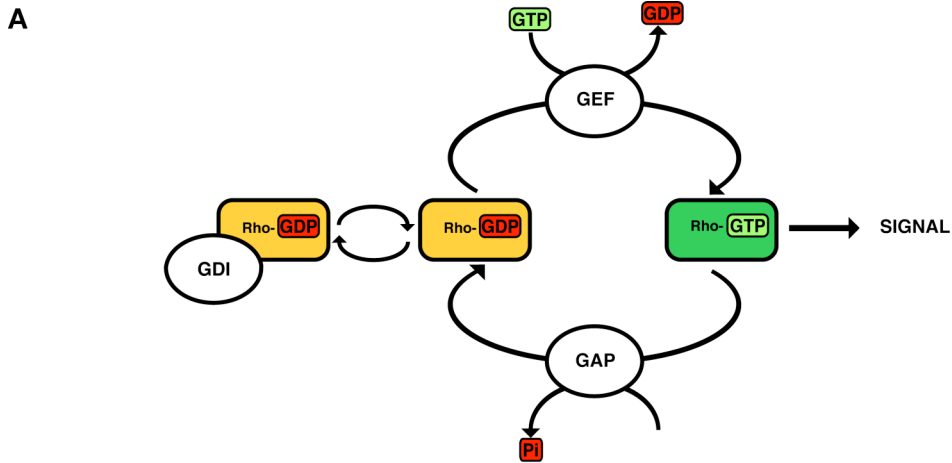
Figure 2. Rho GTPases

(A) Rho GTPase cycle. Rho GTPases cycle between an active GTP-bound state and an inactive GDP-bound state. GEFs activate GTPases by catalyzing the exchange of GDP for GTP. GAPs inactivate by stimulating the intrinsic GTPase activity. GDIs are required to block spontaneous activation. (B) *C. elegans* Rho GTPases and their human orthologs. Percentage of homology between *C. elegans* Rho GTPases (blue) and their human orthologs (grey boxes) as found by sequence homology (adapted from Reverse-proteomic analysis of Rho GTPases regulation by RhoGAPs using AlphaScreen™, PerkinElmer Life and Analytical Sciences Handout).

1.3.7 CDC-42 regulates actin polymerization through the Arp2/3 complex

The Arp2/3 complex consists of seven subunits including two actin-related proteins Arp2 and Arp3 (Welch et al., 1997). The Arp2/3 complex is inducing actin nucleation and by associating laterally on existing filaments it induces filament branches by a characteristic angle of 70 degrees to the host filament (Pollard et al., 2000). This complex is a conserved actin nucleation factor, being present in eukaryotes ranging form yeast to humans (Machesky and Gould, 1999). CDC-42 activates the complex indirectly through members of the Wiskott-Aldrich syndrome protein (WASP) family. CDC-42 activates two members of this family, WASP and N-WASP directly with the lipid PI(4,5)P$_2$ as a cofactor (Rohatgi et al., 1999). WASP family proteins bind to activated CDC-42 through their GBD/CRIB (GTPase-binding domain/Cdc42 and Rac interactive binding) domain. WASP proteins bind to G-actin and the Arp2/3 complex through a region called VCA, causing actin polymerization and elongation. The binding of WASP proteins to other proteins including profilin is thought to enhance actin polymerization (Takenawa and Miki, 2001).

In *C. elegans* embryos, CDC-42 activity is essential. RNAi-mediated depletion of CDC-42 leads to a disruption of cortical polarity (Gotta et al., 2001; Kay and Hunter, 2001). However, the extent to which the underlying acto-myosin cortex is affected in *cdc-42(RNAi)* embryos has not been determined. Cytokinesis takes place in *cdc-42(RNAi)* embryos, suggesting that acto-myosin mediated contractility is present. Disruption of the Arp2/3 complex results in embryonic arrest during morphogenesis in *C. elegans* (Sawa et al., 2003; Severson et al., 2002). In one-cell embryos, depletion of the Arp2/3 complex does not affect cytokinesis. However, membrane blebbing was observed, suggesting that the complex is required for membrane stability (Severson et al., 2002). Later in development the Arp2/3 complex is required for cell migration during ventral closure (Sawa et al., 2003).

1.3.8 RhoA regulates actin polymerization through formin homology proteins

RhoA regulates formin homology proteins, which are important for actin filament nucleation and elongation (Wallar and Alberts, 2003). Formins are defined by the conserved formin homology domain, FH1 and FH2, and have been found to play important roles in cell polarity and cytokinesis. It appears that actin polymerization by formins is stimulated by profilin. Profilin is a G-actin binding protein that accelerates the exchange of ADP to ATP on actin and promotes actin polymerization (Pollard et al., 2000;

Witke, 2004). Profilin interacts with the FH1 domain and is required for formin function. Depletion of the yeast formin proteins and profilin leads to loss of actin cables and depolarized cell growth and also cytokinesis failures (Chang et al., 1997; Haarer et al., 1990; Imamura et al., 1997). Likewise, mutations in both proteins abolishes cytokinesis in *Drosophila* (Giansanti et al., 1998).

The *C. elegans* formin CYK-1 and the profilin PFN-1 are required for the accumulation of actin and NMY-2 at the cortex. Compromising the function of either CYK-1 or PFN-1 by RNAi abolished cortical ruffling and cytokinesis, suggesting that both proteins play a role in assembling the acto-myosin cytoskeleton in the *C. elegans* embryo (Severson et al., 2002; Severson and Bowerman, 2003; Swan et al., 1998).

1.3.9 RhoA promotes the assembly of actin and myosin II into contractile filaments

Our knowledge how actin and non-muscle myosin II (NMY-2) form a contractile network comes from studies on the formation of the contractile ring assembly required for cytokinesis. Myosin II is a motor protein consisting of a parallel dimer of heavy chains, each bound to an essential light chain and a regulatory light chain. Myosin II binds to the actin filament. ATP hydrolysis induces a conformational change in the myosin head driving translocation of actin filaments and the constriction of the contractile ring. Depletion or inhibition of RhoA was shown to block cytokinesis (Aktories and Hall, 1989; Drechsel et al., 1997; Jantsch-Plunger et al., 2000; Kishi et al., 1993; Mabuchi et al., 1993; Moorman et al., 1996; Yuce et al., 2005). RhoA is required for the assembly of actin and myosin II into a contractile meshwork both by controlling actin polymerization through the formin-profilin pathway and by regulating myosin II activity. RhoA controls myosin II activity by promoting phosphorylation of the myosin light chain by the Rho dependent kinase (ROCK) and the citron kinase. Citron kinase phosphorylates the light chain directly, whereas ROCK affects the regulatory light chain by phosphorylating and inhibiting the MLC phosphatase (Glotzer, 2005; Jaffe and Hall, 2005).

As discussed above, the activity of Rho-family GTPases is regulated through GEFs, GAPs, and GDIs. Consistent with the essential role of Rho in cytokinesis, depletion of the RhoGEF ECT-2 in mammalian and *Drosophila* cells (Pebble) blocks cytokinesis (Lehner, 1992; Prokopenko et al., 1999; Tatsumoto et al., 1999; Yuce et al., 2005). Both RhoA and ECT-2 localize to the presumptive cleavage furrow (Tatsumoto et al., 1999; Yuce et al., 2005), and RhoA requires ECT-2 to localize to the cortex. This suggests that ECT-2 recruits and activates RhoA at the cortex, where RhoA promotes the contractile ring assembly.

Depletion of molecules of the RhoA-ROCK pathway, including RhoA (RHO-1), ROCK (LET-502), MLC phosphatase (MEL-11) as well as the regulatory myosin light chain (MLC-4), abolish cytokinesis in *C. elegans* embryos (Jantsch-Plunger et al., 2000; Piekny and Mains, 2002). MEL-11 appeared to regulate the rate of cleavage furrow ingression (Piekny and Mains, 2002). This suggests that RHO-1 controls the furrow formation by regulating myosin II activity through ROCK pathway and actin polymerization through the formin-profilin pathway in the one-cell embryo. The *C. elegans* citron-like genes F59A6.5 and W02B8.2 do not encode kinase domains and RNAi to either gene has no effect on cytokinesis (Piekny and Mains, 2002). The role of the RhoGEF ECT-2 has not yet been studied in *C. elegans* embryos*.*

1.3.10 Activation of the PAR-3/PAR-6/aPKC complex by CDC-42

PAR-6 is a direct target of the activated form of CDC-42 in a variety of cell types including epithelia, neutrophils, neurons and fibroblasts (Etienne-Manneville, 2004). GTP-bound CDC-42 interacts with the semi-CRIB domain of PAR-6 and thereby it induces a conformational change in PAR-6, which leads to the subsequent activation of aPKC (Garrard et al., 2003). Binding of CDC-42 to PAR-6 allows binding to PAR-3. PAR-6 interacts with its single PDZ with the first PDZ domain of PAR-3 (Etienne-Manneville and Hall, 2003b; Henrique and Schweisguth, 2003). Several studies have shown that CDC-42 links the polarity complex to a signaling pathway that controls microtubule dynamics in migrating fibroblast (Stowers et al., 1995), endothelial cells (Tzima et al., 2003) and astrocytes (Etienne-Manneville and Hall, 2001; Etienne-Manneville and Hall, 2003a). Glycogen synthase kinase 3β (GSK-3β) and suppressor adenomatous polyposis coli protein (APC) meditate β-catenin degradation and regulate microtubule stability. CDC-42 activates aPKC (PKCζ) through PAR-6, which leads to the phosphorylation and inactivation of GSK-3β. This in turn allows APC to stabilize microtubules at the leading edge of the migrating cell. This stabilization of microtubules plays a critical role in directed transport of proteins and vesicle for cell polarization (Etienne-Manneville and Hall, 2003a).

In *cdc-42(RNAi)* embryos, PAR proteins were shown to be initially asymmetrically localized, but at two-cell stage, they were found uniformly distributed. This suggested that CDC-42 is involved in maintenance of polarity. Moreover, CDC-42 was shown to

interact with PAR-6 (Gotta et al., 2001) and depletion of CDC-42 affected spindle positioning. In *cdc-42(RNAi)* embryos, the spindle was symmetrically positioned giving rise of two blastomeres equally in size (Gotta et al., 2001; Kay and Hunter, 2001).

1.4 Polarity establishment in *C. elegans*

Several events occur concurrently during the establishment of the anterior-posterior axis in *C. elegans* embryos: the segregation of the acto-myosin cytoskeleton leading to a contractile anterior and a non-contractile posterior domain, the segregation of the PAR proteins into an anterior and a posterior domain, and the occurrence of cytoplasmic flows. Mutations in PAR proteins as well as defects in the acto-myosin cytoskeleton abolish the establishment of the anterior-posterior axis (Cowan and Hyman, 2004a; Schneider and Bowerman, 2003).

1.4.1 PAR protein asymmetry

The *C. elegans* oocyte does not have a predetermined polarity. The sperm entry site determines the posterior pole in the one-cell embryo (Goldstein and Hird, 1996). After fertilization the PAR proteins segregate from an initially uniform distribution into two domains: PAR-3, PAR-6 and aPKC localize anteriorly, (Cuenca et al., 2003; Etemad-Moghadam et al., 1995; Hung and Kemphues, 1999; Tabuse et al., 1998; Watts et al., 1996); whereas PAR-1 and PAR-2 localize to the posterior pole (Boyd et al., 1996; Cuenca et al., 2003; Guo and Kemphues, 1995). PAR-4 and PAR-5 are uniformly present at the cortex and in the cytoplasm (Morton et al., 2002; Watts et al., 2000) (Figure 3A). Mutations in PAR genes disrupt their own asymmetry, the asymmetric mitotic spindle position, ribonucleoprotein particles (P-granules) distribution, and the different fates of the daughter cells. Polarization does not require the male pronucleus (Sadler and Shakes, 2000), but the apposition of the sperm-derived centrosome at the posterior cortex was shown to trigger regression of the anterior PAR proteins and concomitantly, the appearance of the posterior PAR proteins at the posterior cortex (Cowan and Hyman, 2004b; Cuenca et al., 2003; Munro et al., 2004).

1.4.2 Contractile polarity

Another manifestation of anterior-posterior polarity is the establishment of "contractile polarity". At the end of meiosis, small transient cortical ruffles can be seen over the entire cortex. The ruffling ceases in the area where the centrosome became juxtaposed to the posterior cortex (Cheeks et al., 2004; Cowan and Hyman, 2004b; Cuenca et al., 2003; Munro et al., 2004). This smooth area gradually expands towards the anterior until 50% egg-length. A constriction called the pseudocleavage furrow separates the smooth posterior domain from the anterior domain, which remains contractile (Hirsh et al., 1976; Strome, 1986). Fixed sample studies revealed that actin becomes asymmetrically localized in the embryo (Strome, 1986; Strome and Hill, 1988) and suggested that the establishment of contractile polarity is associated with the segregation of the acto-myosin cytoskeleton. More recent studies of imaging the non-muscle myosin II heavy chain (NMY-2) fused to GFP, revealed that initially a uniform contractile meshwork is formed which disassembles in close vicinity to the posterior nucleus/centrosome complex and segregates towards the anterior pole (Munro et al., 2004). The signal inhibiting local contractility appears to come from the centrosome. After depletion of SPD-2 or SPD-5 embryos lack a functional centrosome (Hamill et al., 2002; O'Connell et al., 2000), and NMY-2::GFP segregation did not take place (Munro et al., 2004). The establishment of contractile polarity was not observed (Cowan and Hyman, 2004b).

1.4.3 Cytoplasmic flows

Coincident with the establishment of contractile polarity, large cytoplasmic rearrangements are observed. A flow of cortical yolk granules begins at the posterior pole and moves along the cortex to the pseudocleavage furrow. Cytoplasmic flow directed to the posterior pole replenishes the yolk material that had moved away along the cortex previously (Cheeks et al., 2004; Golden, 2000; Hird and White, 1993). The function of circulating cytoplasm is not clear. It might be required to distribute fate determinants as well as organelles. Cytoplasmic flow is absent in embryos with abolished cortical contractions (Cheeks et al., 2004; Cuenca et al., 2003; Guo and Kemphues, 1996b; Hird and White, 1993; Rappleye et al., 1999; Severson et al., 2002; Swan et al., 1998), indicating that acto-myosin contractility is implicated in generating cytoplasmic flows. The PAR proteins were shown to influence cytoplasmic flows (Cheeks et al., 2004; Munro et al., 2004). In *par-3*, *par-6 and par-4* mutants, the flows were abolished. However, how the PAR proteins achieve this mechanistically is not clear.

1.4.4 Relationship between contractile polarity and PAR polarity

The establishment of the contractile and the PAR domains correlates temporally and spatially. The anterior PAR proteins are confined to the anterior contractile domain, while the posterior PAR proteins are confined to the smooth posterior domain (Cuenca et al., 2003; Munro et al., 2004) (Figure 3B), suggesting that the behavior of the cortical acto-myosin cytoskeleton could be involved in establishment of PAR polarity. Indeed, disruption of the acto-myosin cytoskeleton resulted in loss of cortical contractility and mislocalization of the PAR proteins (Cuenca et al., 2003; Guo and Kemphues, 1996b; Hill and Strome, 1988; Hill and Strome, 1990; Severson and Bowerman, 2003; Shelton et al., 1999). For example, in *nmy-2(RNAi)* embryos contractility was abolished, PAR-2 did not localize to the cortex and PAR-6 remained uniformly at the cortex (Cuenca et al., 2003). Imaging of NMY-2::GFP and GFP::PAR-6 revealed correlating movements of both proteins. Depletion of myosin regulatory light chain (MLC-4) reduced the movement of both proteins and the flow of yolk granules to a similar extent and suggested that the anterior PAR proteins are transported somehow by the acto-myosin cytoskeleton to the anterior (Munro et al., 2004). Mutants in PAR genes did not affect the establishment of contractile polarity (Kirby et al., 1990). This has led to the suggestion that contractile polarity is upstream of PAR polarity and regulates the distribution of the PAR proteins along the cortex.

1.4.5 Asymmetric division

The establishment of the anterior-posterior axis results in a posterior displacement of the mitotic spindle and the polarized distribution of cell-fate determinants along the axis. The first division is asymmetric producing a large anterior daughter cell AB and a smaller P1 cell. The AB cell will mainly form ectoderm, whereas P1 will give rise to the germline, endo- and mesoderm (Bowerman, 2000; Guo and Kemphues, 1996a; Rose and Kemphues, 1998).
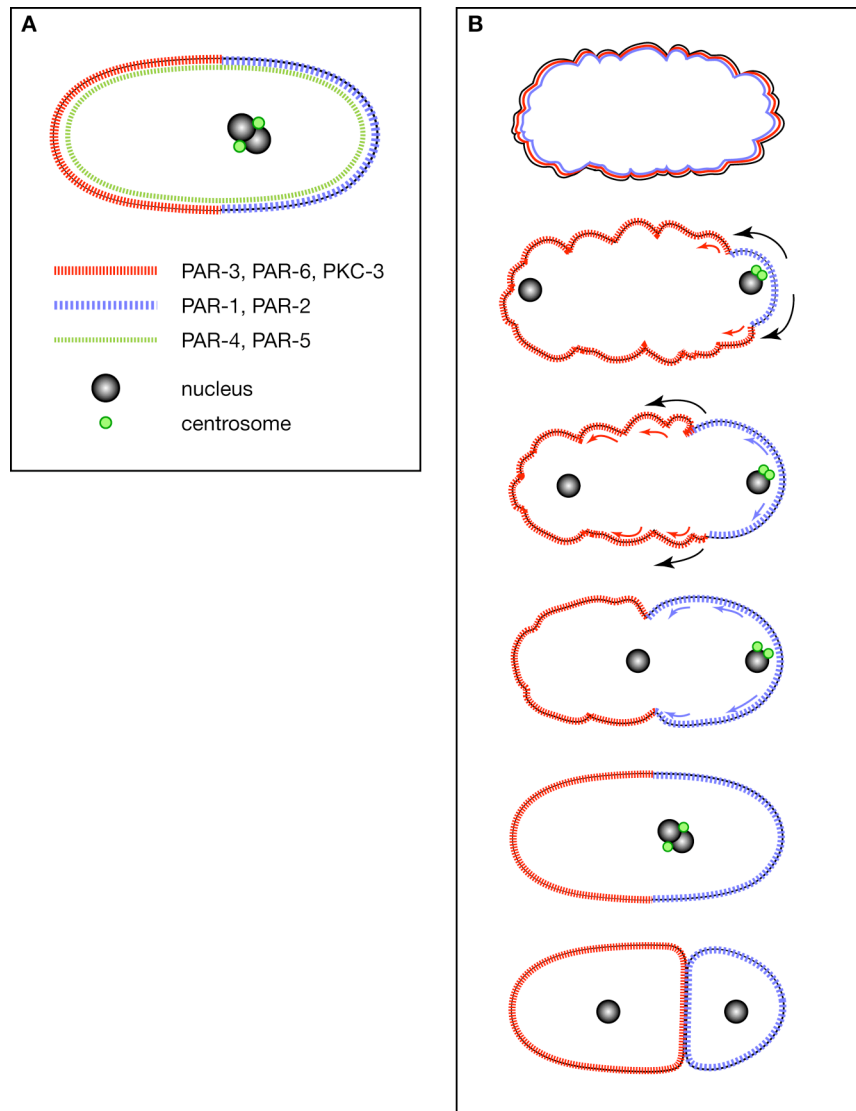
Figure 3. Localization of the PAR proteins in the *C. elegans* embryo

(A) PAR-1 and PAR-2 localize to the posterior cortex. PAR-3, PAR-6 and PKC-3 form a complex in the anterior half of the embryo. PAR-4 and PAR-5 localize uniformly at the cortex and are found in the cytoplasm.

(B) Establishment of contractile polarity and PAR polarity during the first cell cycle. At the end of meiosis, small transient cortical ruffles can be seen over the entire cortex. The ruffling ceases in the area where the centrosome became juxtaposed to the posterior cortex. This smooth area gradually expands towards the anterior until 50% egg-length. PAR-1 and PAR-2 localize to the smooth cortex, whereas PAR-3 and PAR-6 are restricted to the contractile cortex.

1.5 Aim of this PhD thesis

In order to understand polarity establishment in the *C. elegans* embryo, it is important to understand the interplay between the acto-myosin cytoskeleton and the polarity markers, the PAR proteins. It is known that the cytoskeleton is required for the establishment of contractile polarity and for polarized PAR protein distribution, however, how it contributes is unclear. Therefore, it is essential to investigate the dynamics and organization of the acto-myosin cytoskeleton in more detail. The use of tracking programs to follow cortical dynamics in combination with the analysis of the cytoskeletal marker non-muscle myosin II (NMY-2) -GFP, allows a detailed study of the spatial and temporal contribution of the acto-myosin cytoskeleton to polarity formation. To follow polarity formation *in vivo*, time-lapse microscopy of GFP labeled PAR proteins was used. Actin structures can be altered by depleting members of the Rho GTPase family, which are important for actin remodeling. I have chosen CDC-42 and RHO-1 to modulate the acto-myosin cytoskeleton, which allowed me to gain a more detailed picture of the relationship between the cytoskeleton and the PAR proteins. Other Rho GTPases appeared to be dispensable for polarity formation in the one-cell embryo. To further examine how Rho GTPases are implemented in actin remodeling, it is important to analyze how their activity is controlled and how different activities affect polarity formation. For this, two potential regulators of RHO-1, the RhoGEF ECT-2, and the RhoGAP K09H11.3 were analyzed. Both proteins have not yet been studied in the *C. elegans* embryo. The function of CDC-42 in polarity appears to be conserved among different species (Wherlock and Mellor, 2002). It interacts with PAR-6 and was shown to be required for polarization (Gotta et al., 2001; Hutterer et al., 2004; Joberty et al., 2000; Johansson et al., 2000; Lin et al., 2000; Qiu et al., 2000). Detailed analysis of how CDC-42 contributes to polarity is lacking in the *C. elegans* embryo. Therefore, I wanted to clarify how CDC-42 contributes to contractile polarity and PAR polarity in more detail. Furthermore, to understand how CDC-42 as well as RHO-1 contribute to polarity formation, it is essential to analyze their relationship among each other.

This PhD thesis shows that both Rho GTPases CDC-42 and RHO-1 contribute to polarity formation by different mechanisms. The results indicate that the activity of RHO-1 is critical for contractile polarity, which in turn is required for PAR polarity and for linking CDC-42 to the contractile cortex. The role of CDC-42, in contrast, appears to mediate the cortical localization of anterior PAR proteins.

2. RESULTS

2.1 The role of CDC-42 in polarity establishment

2.1.1 CDC-42 is not required for the formation of contractile polarity

CDC-42 was identified as a protein required for polarization of the budding yeast *S. cerevisia* (Adams et al., 1990; Johnson and Pringle, 1990). Impairing the function of CDC-42 resulted in large unbudded cells with disorganized actin cytoskeleton. Further investigations in numerous cell types identified CDC-42 as a universal regulator of the actin cytoskeleton and cell polarity. However, whether CDC-42 also regulates the actin cytoskeleton in *C. elegans* has not been studied. To investigate the potential implication of CDC-42 in actin cytoskeleton regulation in *C. elegans* embryos, it was analyzed whether contractile polarity is established in absence of CDC-42. For this, cortical contractions were tracked over time throughout the establishment of contractile polarity to generate ruffle kymographs (Figure 4; material and methods). In control embryos, the cortex undergoes shallow transient contractions after completion of meiosis. Upon polarization, ruffling ceases at the posterior cortex and this smooth area gradually expands towards the anterior until about 50% egg-length (Figure 4A and 19C). A constriction called the pseudocleavage furrow separates the smooth posterior domain from the anterior domain, which remains contractile (Hirsh et al., 1976; Strome, 1986). Although after *cdc-42(RNAi)* the ruffling was less dynamic and the cortex invaginations were more pronounced, the cortex segregated into a smooth and a contractile domain, as in control embryos (Figure 4B). Thus, the contractile polarity is established after CDC-42 depletion.

2.1.2 CDC-42 is not involved in NMY-2 organization

The establishment of contractile polarity in *cdc-42(RNAi)* embryos was further analyzed by time-lapse imaging of a GFP-tagged marker of the acto-myosin cytoskeleton. NMY-2::GFP exhibits a dynamic pattern of cortical localization during polarity establishment (Munro et al., 2004). *Cdc-42(RNAi)* embryos did not display any obvious structural differences in the NMY-2::GFP network (Figure 12A; Supplemental Movie S1 and S2). The contractile network formed and retracted towards the anterior to form a cap as in control embryos (Figure 12A, t=57, t=545). This finding correlated with the observation that contractile polarity formed after RNAi of *cdc-42* (Figure 4B). Nonetheless, the NMY-2::GFP cap was unstable. While the pseudocleavage furrow was

regressing, small bright foci appeared and moved back towards the posterior (Figure 12A, t=763, t=913). This might suggest that CDC-42 is implicated in stabilizing the acto-myosin network in the anterior half.

2.1.3 CDC-42 is required for the establishment of a PAR-2 domain

The establishment of both the contractile and PAR domains is temporally and spatially correlated. The anterior PAR proteins are confined to the anterior contractile domain, while the posterior PAR proteins are confined to the smooth posterior domain (Cuenca et al., 2003; Munro et al., 2004). Previous studies on fixed samples have shown that in the absence of CDC-42 the PAR proteins are mislocalized (Gotta et al., 2001; Kay and Hunter, 2001), but it was not analyzed further why the PAR localization is defective. To investigate why the localization of PAR proteins is altered, the dynamics of the formation of PAR-2 and PAR-6 domains using GFP fusion proteins were analyzed. In control embryos, GFP::PAR-2 and GFP::PAR-6 are both localized on the cortex until the end of meiosis (Figure 5A, top; data not shown) (Boyd et al., 1996; Cuenca et al., 2003; Etemad-Moghadam et al., 1995; Hung and Kemphues, 1999; Munro et al., 2004); GFP::PAR-2 is then excluded from the cortex (Figure 5A, middle). Consistent with the timing of a putative polarizing signal provided by the centrosome (Cowan and Hyman, 2004b; O'Connell et al., 2000), GFP::PAR-2 reappears exclusively at the posterior pole (Figure 5A, bottom; Supplemental Movie S3), and GFP::PAR-6 segregates towards the anterior pole (Figure 7A). Consistent with previous results from fixed embryos (Gotta et al., 2001; Kay and Hunter, 2001), PAR-2 localized uniformly to the cortex. To investigate in more detail why GFP::PAR-2 is evenly distributed in CDC-42-depleted embryos, GFP::PAR-2 was recorded through the meiotic divisions until the time point at which a GFP::PAR-2 domain was formed in control embryos (Figure 5A and 5B). In contrast to control embryos, GFP::PAR-2 was uniformly distributed on the cortex throughout the meiotic and mitotic cell cycles in *cdc-42(RNAi)* embryos (Figure 5B; Supplemental Movie S4; data not shown).

2.1.4 PAR-2 localization is independent of the centrosome in *cdc-42(RNAi)* embryos

To further investigate why PAR-2 localized uniformly to the cortex throughout cell cycle, it was tested whether the PAR-2 localization in *cdc-42(RNAi)* embryos depends on the presence of a functional centrosome. The centrosome was shown to be essential for polarity establishment (Cowan and Hyman, 2004b; Hamill et al., 2002; O'Connell et al.,

2000). Laser-ablations of the centrosome prior polarity initiation or RNAi of centrosomal proteins including SPD-2 and SPD-5, impaired the formation of a PAR-2 domain. The centrosomal signal appears to be dispensable for meiotic PAR-2 (Cowan and Hyman, 2004b), which suggests that PAR-2 might exists in two different populations: centrosome-independent meiotic PAR-2, and centrosome-dependent PAR-2 localization at the posterior cortex after completion of meiosis. This idea, however, has never been experimentally tested. To investigate whether the PAR-2 localization in *cdc-42(RNAi)* embryos needs the centrosomal signal, CDC-42 was depleted together with SPD-2. In *cdc-42(RNAi);spd-2(RNAi)* embryos, GFP::PAR-2 localized uniformly at the cortex. This result suggests that GFP::PAR-2 localization in *cdc-42(RNAi)* embryos is centrosome-independent and is established during meiosis (Figure 6). Taken together the data suggests that the defect in PAR-2 localization in *cdc-42(RNAi)* embryos results from defects in the removal of PAR-2 from the cortex during the meiotic PAR-2 cycle (Figure 5B).

2.1.5 CDC-42 is required to localize PAR-6 to the cortex

To investigate the function of CDC-42 on PAR-6 localization, time-lapse recordings of GFP::PAR-6 in a *cdc-42(RNAi)* embryo were made (Figure 7; Supplemental Movies S5 and S6). Very reduced amounts of GFP::PAR-6 were observed on the cortex, which were confined to small puncta, suggesting that CDC-42 is required for PAR-6 to localize to the cortex (Figure 7B; Supplemental Movie S4). The small GFP-PAR-6 cortical puncta appeared to localize predominantly to the anterior cortex, further supporting the idea that cortical polarity may establish the asymmetric distribution of PAR-6. CDC-42 is known to interact with PAR-6 (Gotta et al., 2001; Hutterer et al., 2004; Joberty et al., 2000; Johansson et al., 2000; Lin et al., 2000; Qiu et al., 2000), and thus it seems possible that these two proteins act in concert to direct cell polarity, perhaps by removing PAR-2 from the cortex at the end of meiosis. However, how this might be accomplished is still unclear.

2.1.6 CDC-42 localizes anteriorly in the absence of the anterior PAR proteins

To analyze the relationship between CDC-42 and PAR-6 further, we visualized YFP::CDC-42 and investigated its localization in control, *par-6(RNAi)* and *par-3(RNAi),* embryos (Figure 8). In control embryos, prior to polarity establishment, YFP::CDC-42 localized throughout the cortex and was found in ruffles, later in the pseudocleavage

furrow and in the cytokinesis furrow (Supplemental Movie S7). Cortical views revealed that YFP::CDC-42 formed dynamic cable-like structures, which became anteriorly localized during the first cell cycle (Figure 8A and B; Supplemental Movie S8). These cortical structures disorganized around the time of pronuclear rotation and were hardly detectable at the cortex (data not shown). In *par-3(RNAi)* or *par-6(RNAi)* embryos, YFP::CDC-42 still formed the cable–like structures and localized to the anterior cortex, similar to control embryos (Figure 8C-F; Supplemental Movies S9 and S10). This suggests that the anterior localization of YFP::CDC-42 is independent of PAR-3 and PAR-6; however, the localization of GFP::PAR-6 depends on CDC-42 (Figure 7B). Thus, the cortical localization of CDC-42 is upstream of PAR protein localization. In the absence of CDC-42, the anterior PAR proteins fail to localize to the cortex properly and thus, the cell cannot polarize.
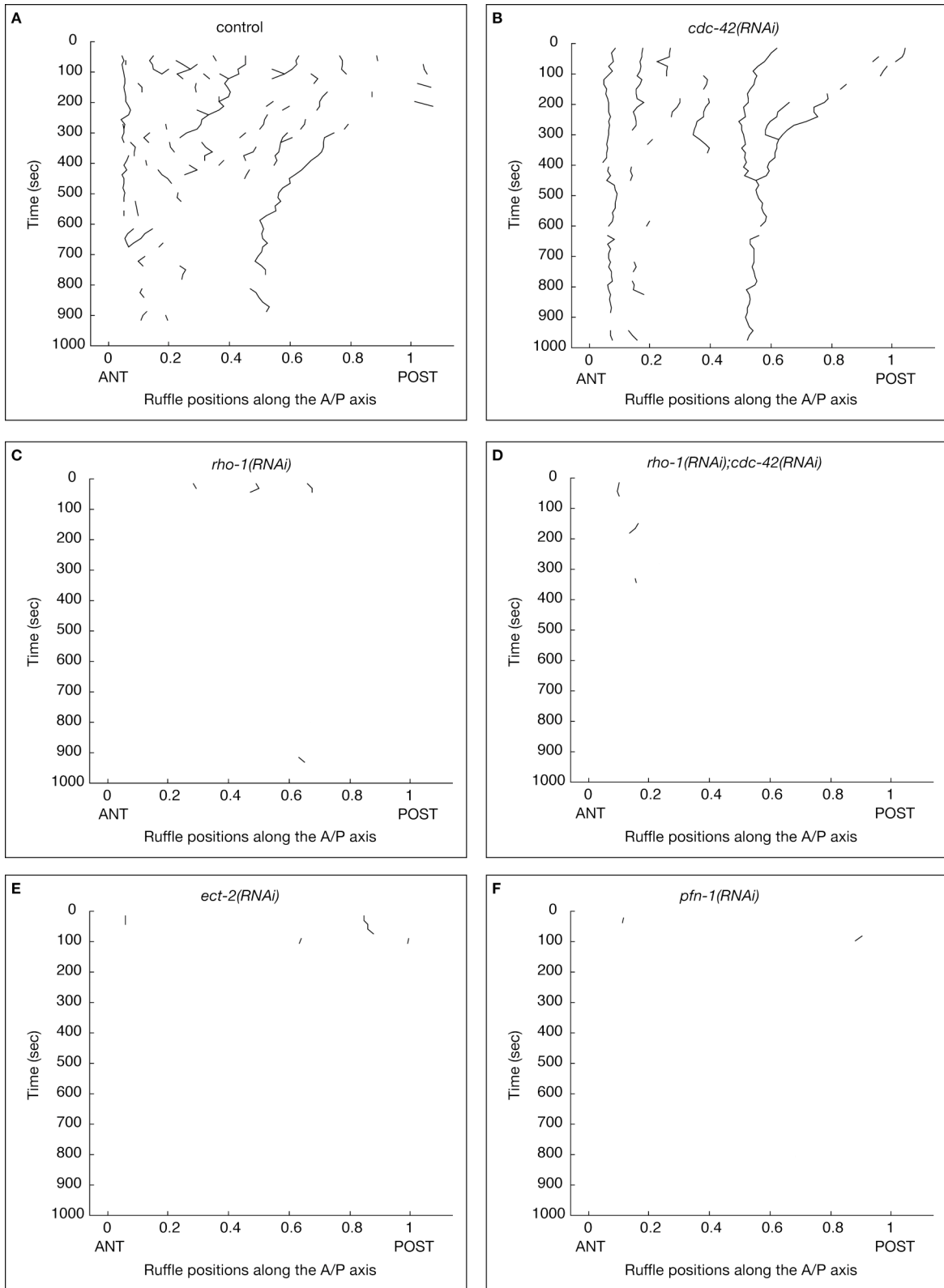
Figure 4. Ruffle kymographs

Figure 4. Ruffle kymographs monitoring the establishment of contractile polarity over time

The position of cortical ruffles along the anterior (ANT)-posterior (POST) axis is projected onto a calculated ellipse. One half of the ellipse was straightened to generate the x-axis (material and methods).

(A) In control embryos the cortex contracts uniformly after completion of meiosis. During anterior-posterior polarity establishment, the posterior cortex becomes cleared from contractions, while the anterior cortex continuous to ruffle.

(B) *Ccd-42(RNAi)* did not prevent the establishment of the contractile polarity. Ruffles were deeper and persisted longer than in control embryos.

(C) *Rho-1(RNAi)*, (D) *cdc-42(RNAi);rho-1(RNAi),* (E) *ect-2(RNAi)* and (F) *pfn-1(RNAi)* abolished contractile polarity establishment.

Figure 5. CDC-42 is required for the PAR-2 localization cycle

Time-lapse images of GFP::PAR-2 polarity establishment in (A) control, (B) *cdc-42(RNAi)* and (C) *rho-1(RNAi)* embryos. Times (sec) are relative to nuclear envelope breakdown. In this and subsequent figures, the embryos are approximately 50 μm in length, the embryo posterior is to the right.

(A) In control embryos GFP::PAR-2 localizes uniformly along the cortex around the time of meiosis (top). After meiosis GFP::PAR-2 disappears from the cortex (middle) and then becomes confined to the posterior pole (bottom).

(B) In *cdc-42(RNAi)* embryos GFP::PAR-2 localized uniformly at the cortex.

(C) *Rho-1(RNAi)* did not affect GFP::PAR-2 localization cycle.
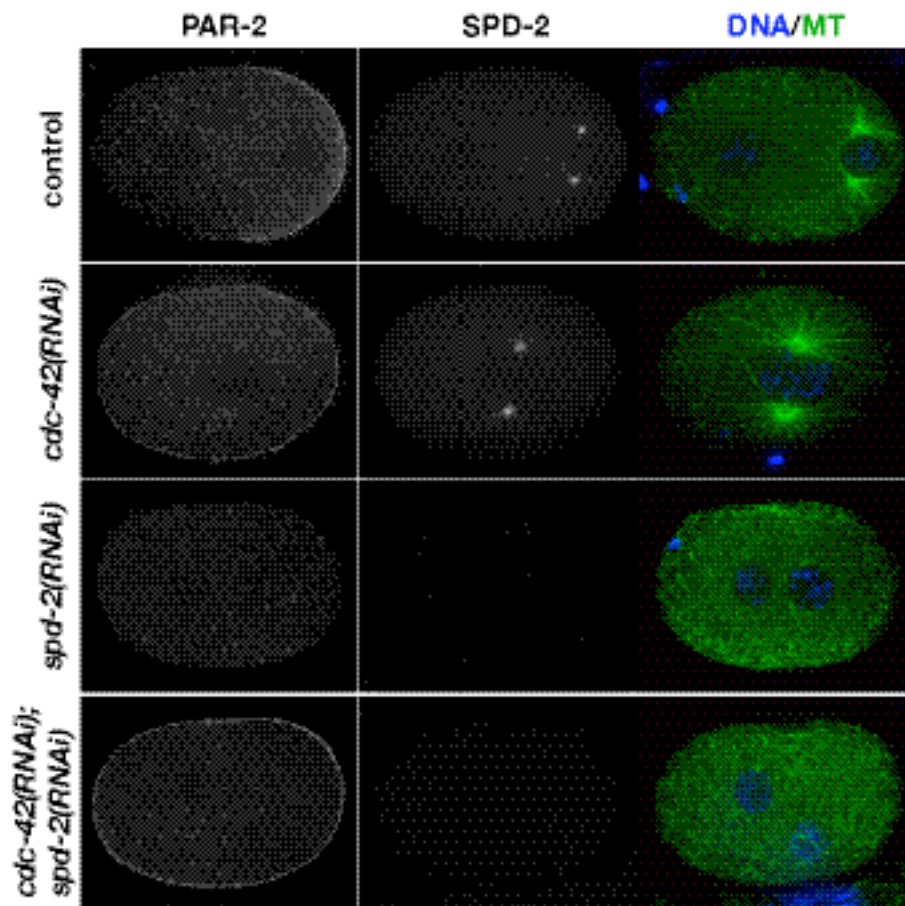
Figure 6. Meiotic GFP::PAR-2 localization is independent of the centrosomal signal

Embryos expressing GFP::PAR-2 were stained for GFP, SPD-2, microtubules (MT, green), and for DNA (blue). In *spd-2(RNAi)* embryos GFP::PAR-2 did not localize to the cortex. In *cdc-42(RNAi);spd-2(RNAi)* embryos, GFP::PAR-2 was found uniformly on the cortex as observed for *cdc-42(RNAi)* alone.
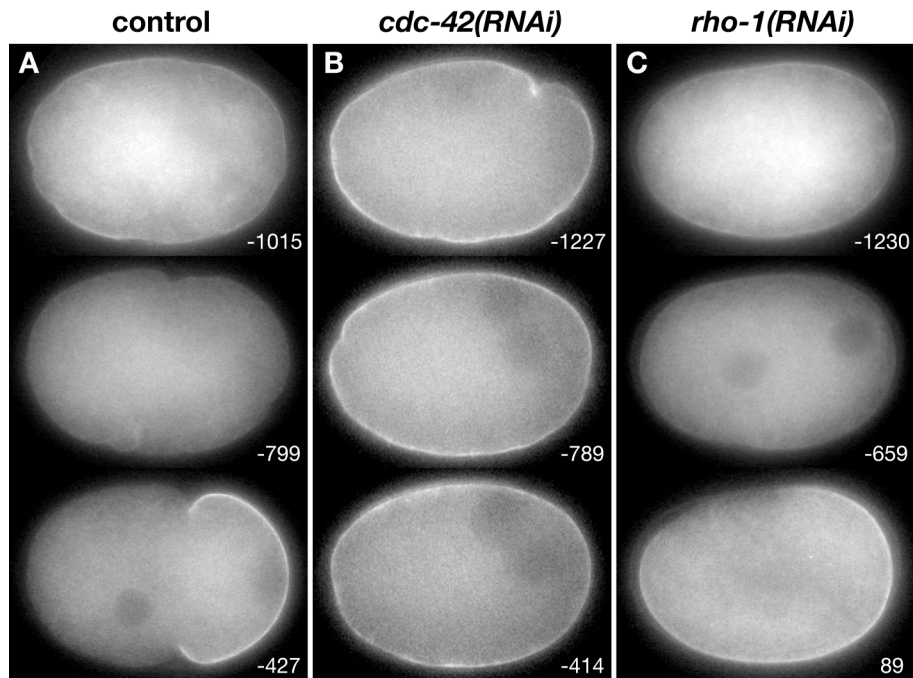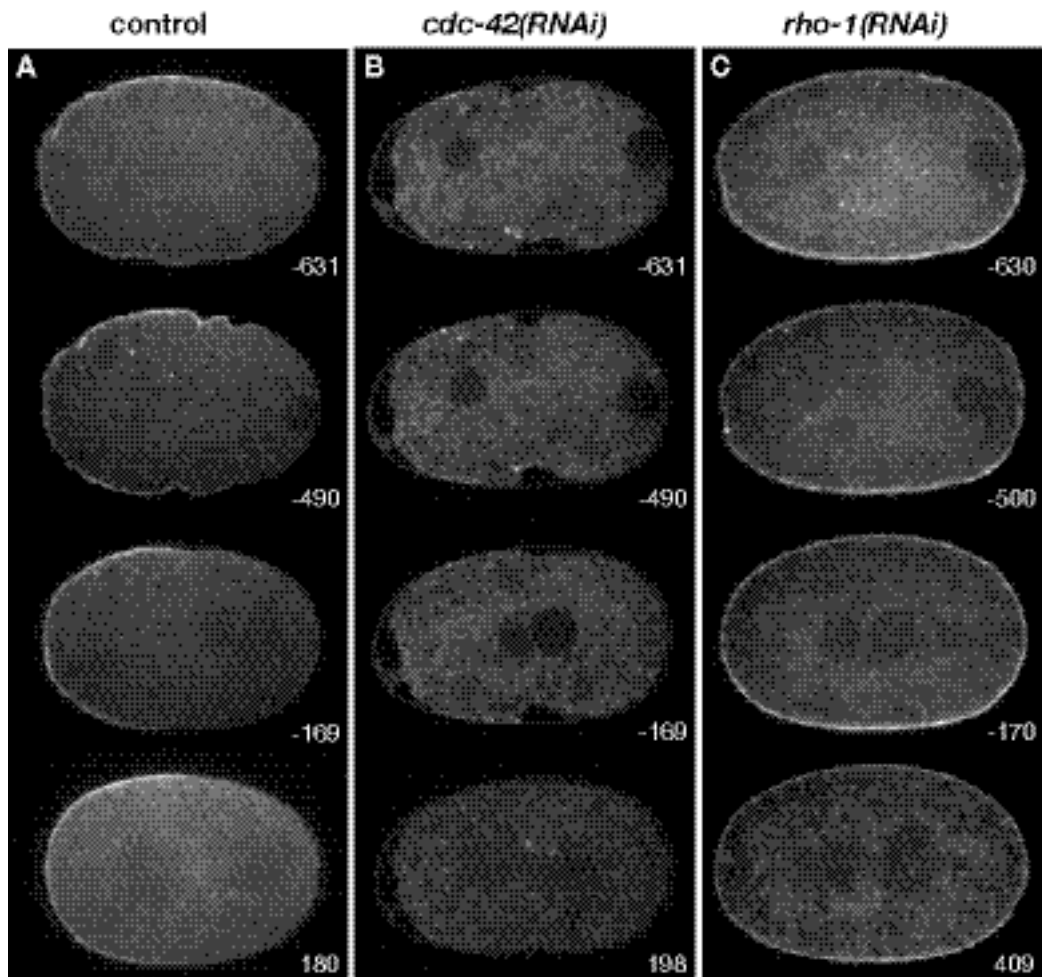
Figure 7. CDC-42 and RHO-1 are required for PAR-6 localization

Time-lapse images of GFP::PAR-6 polarity establishment in (A) control, (B) *cdc-42(RNAi)* and (C) *rho-1(RNAi)* embryos. Times (sec) are relative to nuclear envelope breakdown.

| control | par-3 (RNAi) | par-6 (RNAi) | ect-2 (RNAi) |
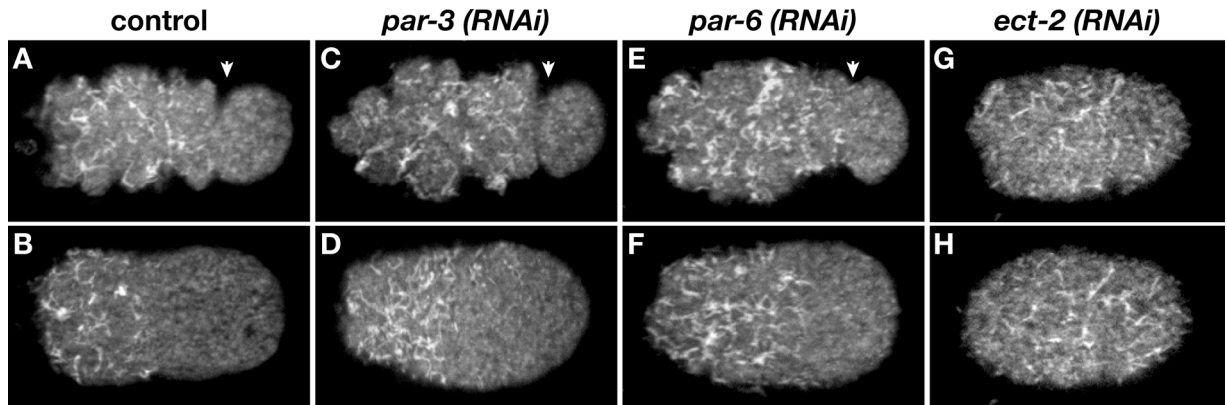
Figure 8. During polarization CDC-42 localization is independent of anterior PAR protein

Cortical views of YFP::CDC-42 in (A, B) control, (C, D) *par-3(RNAi)*, (E, F) *par-6(RNAi)*, (G, F) *ect-2(RNAi)* embryos. Upper panels display embryos in which the pseudocleavage furrow has moved one quarter of embryo length towards anterior (pseudocleavage position is marked by the white arrow). Lower panels show embryos after pseudocleavage regression. In both *par-3(RNAi)* and *par-6(RNAi)* embryos YFP::CDC-42 formes dynamic cable-like structures and concentrates in the anterior cortex. In *ect-2(RNAi)* embryos, YFP::CDC-42 localizes at the cortex, but does not segregate.

2.2 The role of RHO-1 in polarity establishment

The *C. elegans* genome contains only one gene for *rho* (*rho-1*), which shows 87.6% amino acid sequence identity to human RhoA (Chen and Lim, 1994). The role of *C. elegans* RHO-1 in the establishment of embryonic polarity has not been analyzed. To investigate how RHO-1 contributes to polarity establishment, cortical contractions were tracked over time and PAR distribution was analyzed by making time-lapse recordings of GFP::PAR-2 and GFP::PAR-6.

2.2.1 RHO-1 is required for contractility

After depletion of RHO-1 function by RNAi, the embryos fail to undergo cytokinesis, as previously shown (Jantsch-Plunger et al., 2000). Furthermore, other actin-dependent processes such as cortex ruffling, the formation of a pseudocleavage furrow were abolished (Figure 4C) and polar body extrusion often failed. This shows that RHO-1 functions in several aspects of cortical contractility.

2.2.2 RHO-1 is required to form the boundary between anterior and posterior PAR domains

To investigate whether the lack of contractile activity affects PAR localization in *rho-1(RNAi)* embryos, time-lapse images of GFP::PAR-2 and GFP::PAR-6 were made. After RHO-1 depletion, GFP::PAR-6 remained localized throughout the cortex during the entire first cell cycle (Figure 7C; Supplemental Movie S11). In addition, two classes of defects with respect to GFP::PAR-2 localization were observed. For some embryos, GFP::PAR-2 did not localize to the cortex and appeared to remain in the cytoplasm (data not shown). In the remaining embryos, GFP::PAR-2 accumulated and expanded along the cortex and gave rise to a large GFP::PAR-2 domain (Figure 9B; Supplemental Movie S12). The two classes of defects observed may reflect different RHO-1 activity. In the embryos in which PAR-2 localized to the cortex, the GFP::PAR-2 domain correlated with the position of the nucleus-centrosome complex, but the boundary between the GFP::PAR-6 and the GFP::PAR-2 cortical domains failed to form.

2.2.3 Depletion of the Rho GEF ECT-2 results in similar phenotype as *rho-1(RNAi)*

To confirm the role of RHO-1 activity in establishment of polarity, the function of T19E10.1, a potential Rho guanine nucleotide exchange factor (RhoGEF) was investigated. Sequence analysis revealed that T19E10.1 is the *C. elegans* homolog of the Drosophila Pebble (DmPebble) and of the human ECT2 (HsECT-2) (42% similarity on protein level, Bianca Habermann, personal communication); both have been shown to activate RhoA signaling (Prokopenko et al., 1999; Tatsumoto et al., 1999). RhoGEFs activate GTPases by catalyzing the exchange of GDP for GTP. Therefore, RNAi of T19E10.1 should phenocopy the defects following RHO-1 depletion. Analysis of cortical ruffling (Figure 4E), GFP::PAR-2 (Figure 9D and E; Supplemental Movies S13 and S14) and GFP::PAR-6 localization (Supplemental Movie S15) in *T19E10.1(RNAi)* embryos revealed a similar phenotype to *rho-1(RNAi)*. Therefore, this RhoGEF was named ECT-2.
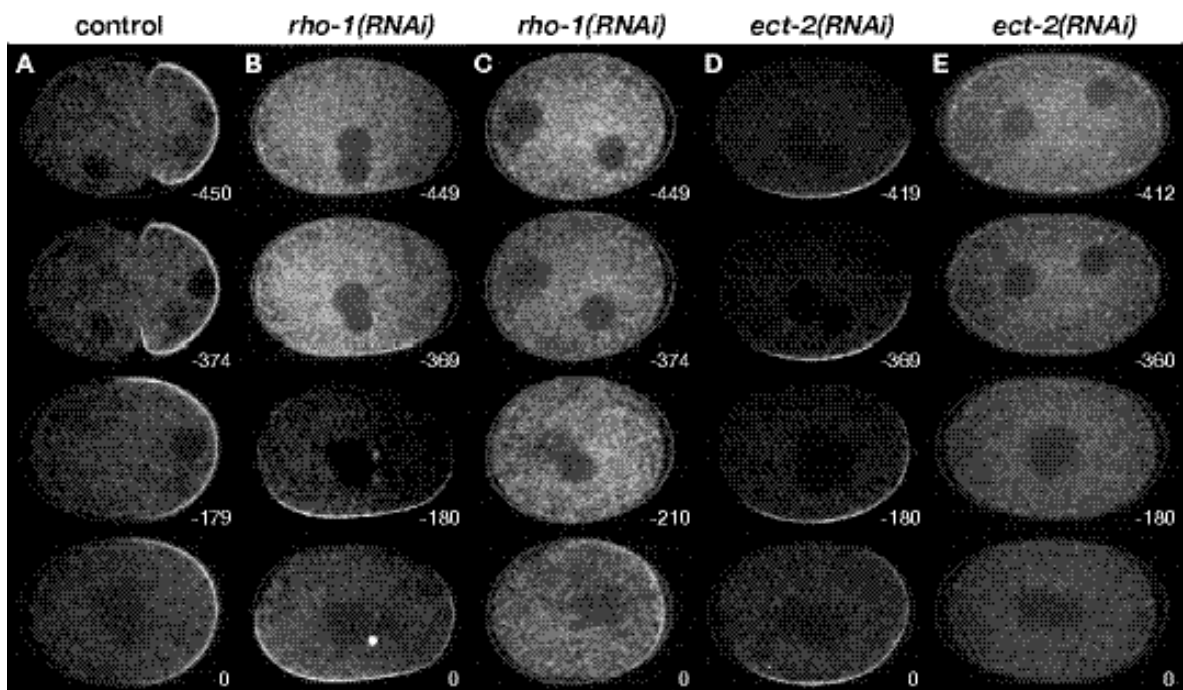
Figure 9. RHO-1 is involved in regulating the PAR-2 domain size

Time-lapse images of GFP::PAR-2 polarity establishment in (A) control, (B, C) *rho-1(RNAi)*, (D, E) *ect-2(RNAi)* embryos. Times (sec) are relative to nuclear envelope breakdown. *Rho-1(RNAi)* and *ect-2(RNAi)* embryos display similar phenotypes and fall into two classes based on their GFP::PAR-2 localization. (B, D) GFP::PAR-2 spreads along the cortex, resulting in a large GFP::PAR-2 domain. (C, E) GFP::PAR-2 appears late (C) or never at the cortex (E).

2.2.4 *rho-1(RNAi)* and *ect-2(RNAi)* affects timing and size of PAR-2 domain formation

The formation of the GFP::PAR-2 domain in *rho-1(RNAi)* and *ect-2(RNAi)* embryos was analyzed in more detail. First, the appearance of GFP::PAR-2 at the cortex relative to nuclear envelope breakdown (NEBD) was measured (Figure 10A). In control embryos, GFP::PAR-2 appears at 14.15 ± 1.92 min before NEBD (n=8); however, in *rho-1(RNAi)* and in *ect-2(RNAi)* embryos GFP::PAR-2 localization to the cortex varied with time and was delayed (Figure 10, 9B and C). On average, in *rho-1(RNAi)* embryos the localization took place at 4.19 ± 1.71 min before NEBD (n=5) and in *ect-2(RNAi)* embryos at 4.72 ± 3.64 min before NEBD (n=6), respectively. This suggested that the correct timing of GFP::PAR-2 domain establishment requires RHO-1 activity.

In contrast to *cdc-42(RNAi)*, the GFP::PAR-2 localization cycle was not impaired neither in *rho-1(RNAi)* embryos (Figure 5C; Supplemental Movie S12) nor in *ect-2(RNAi)* embryos (Supplemental Movie S13), indicating that CDC-42 acts prior to RHO-1 in determining PAR-2 localization.

In a next step, the extent of the PAR-2 domain in *rho-1(RNAi)* embryos was measured by calculating the maximal extent of the GFP::PAR-2 domain as a fraction of the embryo circumference (Figure 10B). In control embryos, GFP::PAR-2 reached maximal domain extension directly after pseudocleavage furrow regression, about 53 ± 2% of the embryo circumference (n=8). In *rho-1(RNAi)* embryos, the extent of GFP::PAR-2 was on average greater than in control embryos (about 70 ± 15% of the circumference, n=10) (Figure 10B and 9B). Similar results were seen after RNAi of *ect-2* (data not shown; Figure 9D).

A Appearance of GFP::PAR-2 at the cortex relative to NEBD

B
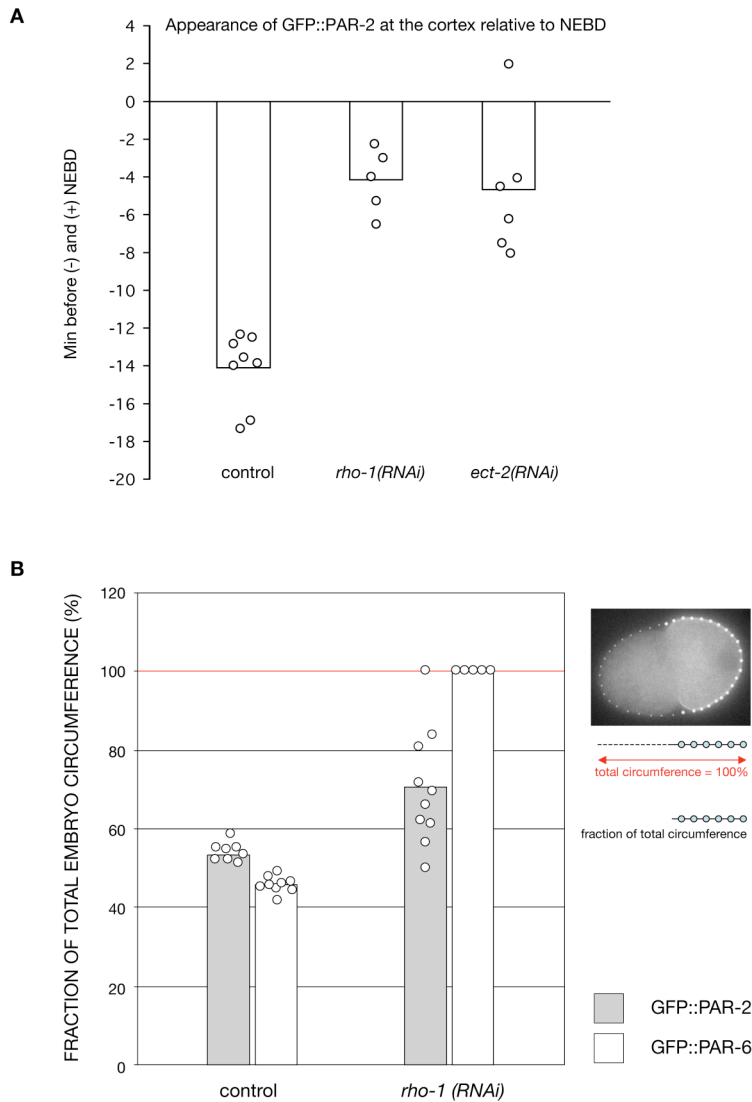
Figure 10. RHO-1 is required for the correct timing of PAR-2 domain establishment and controls PAR-2 domain size

(A) Appearance of GFP::PAR-2 at the cortex relative to nuclear envelope breakdown (NEBD). In control embryos, GFP::PAR-2 appears at the cortex at 14.15 ± 1.92 min before NEBD. GFP::PAR-2 localization to the cortex was delayed in both *rho-1(RNAi)* (4.19 ± 1.71 min before NEBD) and in *ect-2(RNAi)* (4.72 ± 3.64 min before NEBD) embryos. (B) The GFP::PAR-2 domain size was manually tracked after the GFP::PAR-2 domain reached its maximal extent, whereas the GFP::PAR-6 domain was tracked after pseudocleavage regression. The domain size was calculated as a fraction of the embryo circumference. In control embryos, the GFP::PAR-2 domain extent amounts to 53 ± 2% (n=8); GFP::PAR-6 domain to 46 ± 2% (n=9). In *rho-1(RNAi)* embryos, GFP::PAR-2 domain extent amounts to 70 ± 15% (n=10), whereas GFP::PAR-6 is uniformly distributed along the cortex (100%, n=5).

2.2.5 Analysis of cortical flows in *rho-1(RNAi)* embryos

Coincident with the establishment of contractile polarity large cytoplasmic rearrangements are observed. Yolk granules in close proximity to the cortex move towards the anterior pole, whereas internal cytoplasm flows to the posterior pole replenishing the yolk material that had moved away along the cortex previously. The cytoplasmic streaming of yolk granules is thought to be created by the anterior segregation of the acto-myosin cytoskeleton (Cheeks et al., 2004; Golden, 2000; Hird and White, 1993; Munro et al., 2004). To test whether cytoplasmic flows require RHO-1 activity, cortical flow of yolk granules was analyzed by generating kymographs from differential interference contrast (DIC) and GFP::PAR-2 time-lapse recordings during polarity establishment (Figure 11). The results show that the appearance of GFP::PAR-2 at the cortex is associated with cortical flows (Cheeks et al., 2004). After *ect-2(RNAi)*, cortical flows occurred along the cortex while the GFP::PAR-2 domain was extending (Figure 10B. In *ect-2(RNAi)* embryos in which GFP::PAR-2 did not localize to the cortex, no flows were observed (Figure 11C). Thus, in *ect-2(RNAi)* embryos cytoplasmic flows are associated with the presence of the cortical PAR-2 domain, as observed in control embryos. Similar results were seen after *rho-1(RNAi)* (data not shown). This lead to the suggestion that in the absence of contractile polarity, cytoplasmic flows can still occur. Interestingly, the flows are separable from the segregation of the anterior PAR domain in *ect-2(RNAi)* embryos.

2.2.6 RHO-1 is required for NMY-2 organization and dynamics

The analysis of *rho-1(RNAi)* embryos suggests that RHO-1 is required in some way to establish the boundary between the posterior and the anterior PAR domains. In *rho-1(RNAi)* embryos, GFP::PAR-6 remains uniformly distributed throughout the cortex, while GFP::PAR-2 spreads onto the cortex, overlapping with the GFP::PAR-6 domain. Overlapping posterior and anterior PAR domains have been previously reported for RNAi of *nmy-2* (Cuenca et al., 2003; Guo and Kemphues, 1996b), *mlc-4* (Shelton et al., 1999) and *par-5* (Cuenca et al., 2003; Morton et al., 2002), indicating that organization of the acto-myosin cytoskeleton may be important for establishing the boundary between the PAR proteins. To investigate in more detail the requirement of RHO-1 in cortical contractility, NMY-2::GFP (Munro et al., 2004) was used to monitor myosin organization and dynamics by time-lapse microscopy (Figure 12; Supplemental Movie S1).

In early control embryos, NMY-2::GFP forms first a dynamic network throughout the entire cortex consisting of foci clusters interconnected by small filaments (Figure 12A, t=54). In close vicinity to the posterior nucleus/centrosome complex, the NMY-2::GFP network begins to disassemble and coincidently segregates towards the anterior half (Munro et al., 2004). During this process, the NMY-2::GFP foci clusters become concentrated into an anterior cap, while the posterior half becomes devoid of detectable NMY-2::GFP foci (Figure 12A, t=450). By the time the anterior cap is formed, the original foci clusters disappear, and subsequently numerous smaller foci in a dense pattern emerge (Figure 12A, t=750). Reducing the function of either RHO-1 or ECT-2 by RNAi altered the NMY-2::GFP organization drastically (Figure 12A; Supplemental Movie S16; data not shown). The early network of interconnected foci clusters did not form. Instead, small foci were uniformly distributed throughout the cortex (Figure 12A, t=54), reminiscent of small foci formed after the establishment of the anterior cap in control embryos (Figure 12A, t=750, 914). These foci collectively segregated away in the same direction at similar speeds (average velocity 0.17 μm/sec, n=10) in an *ect-2(RNAi)* embryo (Figure 12C).

To further investigate the relationship between NMY-2::GFP segregation and GFP::PAR-2 appearance at the cortex, a strain expressing both NMY-2::GFP and GFP::PAR-2 was constructed. In wild type embryos, NMY-2::GFP migrated away from the GFP::PAR-2 domain concomitant with GFP::PAR-2 localization to the cortex (Figure 12B; Supplemental Movies S17 and S18). *rho-1(RNAi)* and *ect-2(RNAi)* embryos also displayed a coordinated anterior-directed segregation of NMY-2-GFP and posterior localization of GFP-PAR-2. My analysis of PAR-6 distribution in *rho-1(RNAi)* and *ect-2(RNAi)* embryos indicated that GFP::PAR-6 does not segregate into a cortical domain (Figure 7C; Supplemental movies S14 and S15). Taken together, this data shows that RHO-1 depletion separates the segregation of NMY-2::GFP from the movement of GFP::PAR-6, suggesting that RHO-1 is involved in organizing NMY-2::GFP into the early network of foci clusters, which could be important for GFP::PAR-6 segregation.
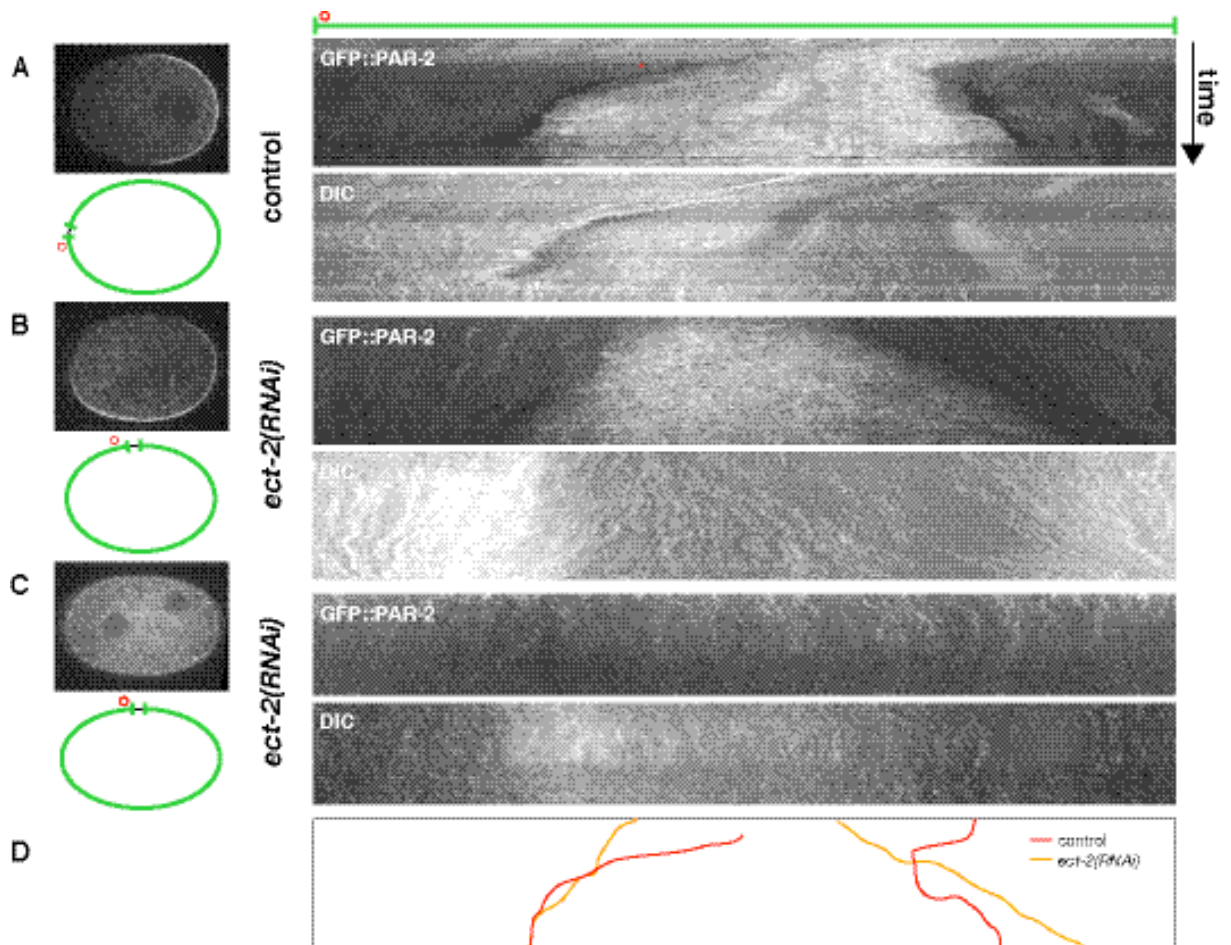
Figure 11. Flows correlate with PAR-2 appearance at the cortex

Kymographs of time-lapse DIC (monitors yolk granule movement) and GFP::PAR-2 recordings of (A) control, (B) *ect-2(RNAi)* embryos with GFP::PAR-2 localizing to the cortex and (C) *ect-2(RNAi)* embryos without cortical GFP::PAR-2. Kymographs were made from a curved line along the embryo cortex (green line), centered on the location of initial PAR-2::GFP appearance. The red circle marks the left side of the kymographs. (D) Overlay of the border of GFP::PAR-2 domain from the kymograph of (A) control (in red) and of (B) *ect-2(RNAi)* (in yellow).
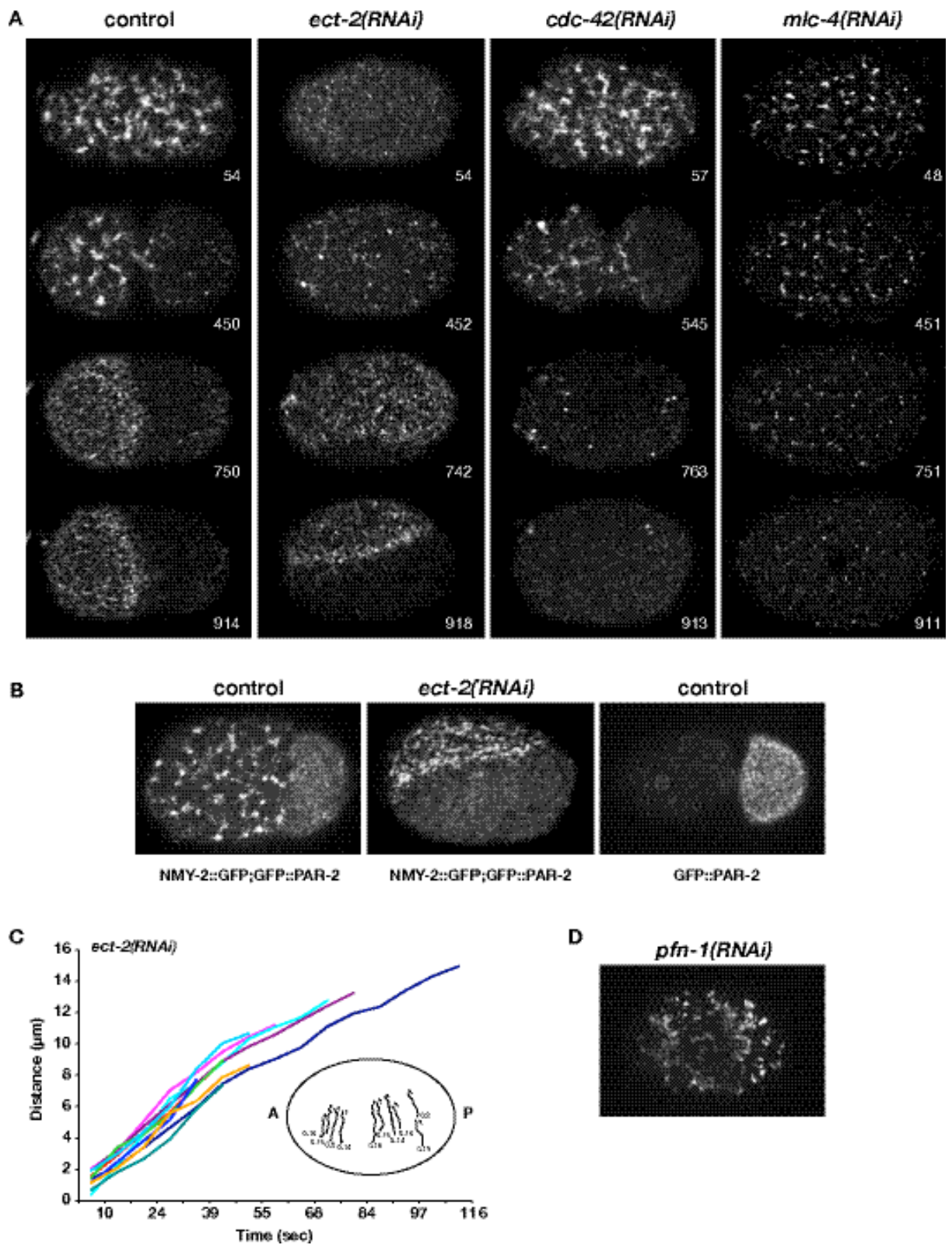
Figure 12. RHO-1 activity organizes NMY-2 into foci clusters, and uncouples NMY-2 segregation from PAR-6 segregation.

Figure 12. RHO-1 activity organizes NMY-2 into foci clusters and uncouples NMY-2 segregation from PAR-6 segregation

Time-lapse images (surface view) of GFP::NMY-2 during polarity establishment of (A) control, *ect-2(RNAi)*, *cdc-42(RNAi)* and *mlc-4(RNAi)* embryos. Times (sec) are relative to pronuclei appearance. (B) Images of the combined NMY-2::GFP;PAR-2::GFP line (surface view) of a control (left) and an *ect-2(RNAi)* embryo (middle). Cortical view of GFP::PAR-2 (right). GFP::PAR-2 labels the posterior cortex. (C) Tracking of NMY-2::GFP foci in an *ect-2(RNAi)* embryo. The small foci moved concomitantly at the same time and with similar velocities (average velocity = 0.17 µm/sec). (D) Cortical view of GFP::NMY-2 in *pfn-1(RNAi)* embryo.

2.2.7 CDC-42 segregation depends on RHO-1 activity

This study showed that RHO-1 is required to link the segregation of PAR-6 to the retraction of NMY-2 towards the anterior. In *rho-1(RNAi)* embryos, NMY-2 segregates but PAR-6 does not. Furthermore, it was shown above that CDC-42 may be required to effectively link PAR-6 to the cortex (Figure 7) and that CDC-42 segregates to the anterior cortex during polarity establishment. I wanted to determine if RHO-1 depletion affected the link between PAR-6 and CDC-42 or the link between CDC-42 and the cortex. To asses whether CDC-42 localizes to the cortex in the absence of RHO-1 activity, ECT-2 was depleted and YFP::CDC-42 distribution at the cortex was analyzed. YFP::CDC-42 localized independently of RHO-1 activity to the cortex, but the segregation to the anterior was impaired (Figure 8G and H; Supplemental Movie S19). The localization of CDC-42 in *rho-1(RNAi)* embryos is similar to the localization of PAR-6 in *rho-1(RNAi)* embryos, suggesting that RHO-1 may regulate the association of CDC-42 with the acto-myosin cortex, and that CDC-42, in turn, localizes PAR-6 to the cortex.

2.2.8 Depletion of the RHO-1 target proteins PFN-1 and MLC-4 result in defects similar to *rho-1(RNAi)*

In budding yeast, formins and profilin are effectors of active RhoA and are essential for transducing the rho signal to the actin cytoskeleton (Dong et al., 2003). Depletion of the *C. elegans formin* CYK-1 and proflin PFN-1 abolished ruffling and cytokinesis (Severson et al., 2002; Severson and Bowerman, 2003; Swan et al., 1998). To test whether RHO-1 acts on the cytoskeleton through the formin-profilin pathway during polarity formation, PFN-1 was depleted and cortical dynamics and PAR polarity was analyzed. *pfn-1(RNAi)*

embryos displayed a strong *rho-1(RNAi)* phenotype: Every aspect of cortical activity was abolished (Figure 4F), GFP::PAR-2 did not localize to the cortex, and GFP::PAR-6 did not segregate (Figure 13). Similarly, the in *mlc-4(RNAi)* embryos PAR-2 was compromised into a small domain, whereas GFP::PAR-6 remained uniformly distributed (data not shown). The analysis of the NMY-2::GFP organization showed that the NMY-2 meshwork was defective in both *pfn-1(RNAi)* and *mlc-4(RNAi)* embryos. NMY-2::GFP formed irregular shaped aggregates (Figure 13D), which moved unidirectionally in *pfn-1(RNAi)* embryos. In *mlc-4(RNAi)* embryos the NMY-2::GFP foci were smaller (Figure 12A). NMY-2::GFP segregation did not take place at any time after depletion of either PFN-1 or MLC-4. These results show that the establishment of polarity requires the acto-myosin cytoskeleton. The phenotypic similarity between *pfn-1(RNAi)*, *mlc-4(RNAi)* and *rho-1(RNAi)* embryos with respect to cortical polarity suggests that RHO-1 may regulate the acto-myosin cytoskeleton and myosin II activity during polarity establishment through the formin-profilin pathway and by the ROCK pathway, respectively.
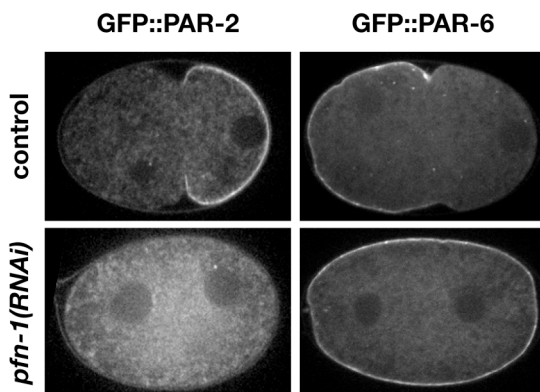
Figure 13. *pfn-1(RNAi)*

2.3 Relationship between CDC-42 and RHO-1

2.3.1 RHO-1 and CDC-42 act in separate pathways to control polarity establishment

To investigate whether CDC-42 acts in the same pathway as RHO-1 in polarity establishment, both CDC-42 and RHO-1 were depleted at the same time and cortical ruffling (Figure 4D) as well as GFP::PAR-2 and GFP::PAR-6 distribution from time-lapse movies was analyzed (Figure 14). In *cdc-42(RNAi); rho-1(RNAi)* embryos, the GFP::PAR-2 cycle failed and GFP::PAR-6 localization was reduced to puncta, similar to *cdc-42(RNAi)* embryos. However, like the *rho-1(RNAi)* embryos, the contractile activity of the cortex was lost following double depletion of RHO-1 and CDC-42 (Figure 4D; Supplemental Movies S20 and S21). Since the single *cdc-42(RNAi)* and *rho-1(RNAi)* phenotypes appear to be additive when both proteins are depleted, it seems that CDC-42 and RHO-1 work in separate pathways to control polarity establishment.

GFP::PAR-2 **GFP::PAR-6**

cdc-42(RNAi); rho-1(RNAi) *cdc-42(RNAi); rho-1(RNAi)*
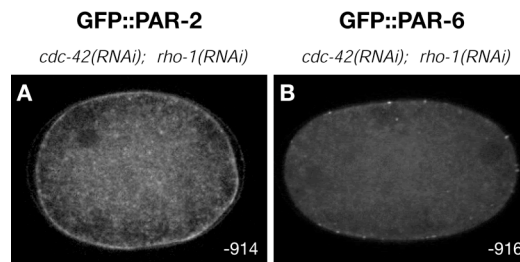
Figure 14. RHO-1 and CDC-42 act in separate pathways to control polarity establishment. Time-lapse images of GFP::PAR-2 and GFP::PAR-6 during polarity establishment in *cdc-42(RNAi);rho-1(RNAi)* embryos. Times (sec) are relative to nuclear envelope breakdown.

A

	control	rho-1(RNAi)	cdc-42(RNAi)
ruffling	+	-	+
posterior smoothing	+	-	+
PSCF	+	-	+
cytokinesis	+	-	symmetric
PAR-2 localization	asymmetric	large asymmetric domain or no PAR-2	uniform
PAR-6 localization	asymmetric	uniform	very reduced
NMY-2 organization	foci clusters and small foci	small foci	foci clusters and small foci

B

	NMY-2::GFP			GFP::PAR-2/PAR-6	
	foci clusters	small foci	segregation	PAR-2 present	PAR-6 uniform
control	+	+	+	+	_
cdc-42(RNAi)	+	+	+	+	_
rho-1(RNAi)	-	+	+/-	+/-	+
nmy-2(RNAi)	-	-	-	+/-*	+*
mlc-4(RNAi)	-	-	-	+/-**	+
pfn-1(RNAi)	-	-	-	-	+
spd-5(RNAi)	+	-	-	-	+

Figure 15

(A) Comparison of rho-1(RNAi) with cdc-42(RNAi) phenotype. (B) Summary of different RNAi phenotypes (Abbreviations: PSCF pseudocleavage furrow, * Cuenca et. al., 2003, ** Carrie Cowan, personal communication).

2.4 Identification and characterization of the RhoGAP K09H11.3

The regulation of Rho GTPases by GEFs and GAPs is critical for their temporal and spatial localized activation. To understand how Rho GTPases regulate certain processes in the cell, it is important to identify GEFs and GAPs for the respective GTPase. The analysis of the GEF ECT-2 suggested that this might be the only GEF acting on RHO-1, as depletion of ECT-2 appeared to abolish all RHO-1 activity. The identification of a GAP would help to gain more insight into the effect of RHO-1 or CDC-42 activity in the relationship between cortical dynamics and PAR protein distribution. By searching through the genome-wide RNAi database (Sonnichsen et al., 2005) for Rho GAPs displaying defects in cortical contractility, the gene K09H11.3 was identified.

The presence of a single GAP domain similar to Rho GAP domains suggested that K09H11.3 is a potential GAP for Rho GTPases. The *C. elegans* genome contains a putative paralog, Y75B7AL.4, which shows 79 % amino acid identity to K09H11.3. To avoid RNAi cross-silencing as a result of high similarity between the two proteins, three different RNAs were made to distinguish between the proteins. Two short RNAs specific to regions in which both genes differed most were created. The third RNA covered a 500 base pair long sequence in which both proteins were almost identical on nucleotide level. RNAi with the short RNA for K09H11.3 and the long RNA covering both proteins resulted in identical phenotypes. However, RNAi with the short RNA specific to Y75B7AL.4 gave no phenotype, which suggested that Y75B7AL.4 does not play a role in the one-cell embryo and was therefore not analyzed further.

2.4.1 Phylogenetic analysis of K09H11.3

Phylogenetic analysis revealed K09H11.3 is a putative sequence orphan. The *Drosophila melanogaster* RhoGAP54D (DmCG4677) (Figure 16) is the closest homolog to K09H11.3, showing 26 % amino acid sequence identity only to K09H11.3 GAP domain (Bianca Habermann, personal communication). Depletion of RhoGAP54D in Drosophila mushroom body neurons resulted in no obvious phenotype (Billuart et al., 2001).

Figure 16. Rho GAP family phylogenetic tree based on the sequence homology of the K09H11.3 GAP domain.

2.4.2 K09H11.3 localizes to cortex and centrosomes

To address the spatial and temporal expression of the K09H11.3 protein, immunofluorescence studies using an antibody against a peptide corresponding to the C-terminus of K09H11.3 protein were performed. The K09H11.3 antibody labeled the cortex of oocytes but was absent in sperms (data not shown). In fertilized embryos, K09H11.3 antibody localized uniformly to the cortex and to centrosomes (Figure 17). The centrosomal localization was most apparent after the centrosomes had separated. During cell division, K09H11.3 localized to the ingressing cleavage furrow (data not

shown) and localized to the membrane between the blastomeres. In addition, a diffuse cytoplasmic labeling throughout the first cell cycle was observed. On the centrosomes, K09H11.3 appeared to concentrate in a donut-shaped region in a similar pattern to what has been reported for AIR-1 (Hannak et al., 2001) (Figure 18A). However, an overlay of both localization patterns at metaphase revealed that both only partially overlap and that K09H11.3 does not localize to the base of astral microtubules as it was reported for AIR-1 (Hannak et al., 2001) (Figure 18A, inset). The localization pattern of K09H11.3 antibody is proofed to be specific, since in *K09H11.3(RNAi)* embryos no detectable K09H11.3 antibody labeling was observed (Figure 18B).
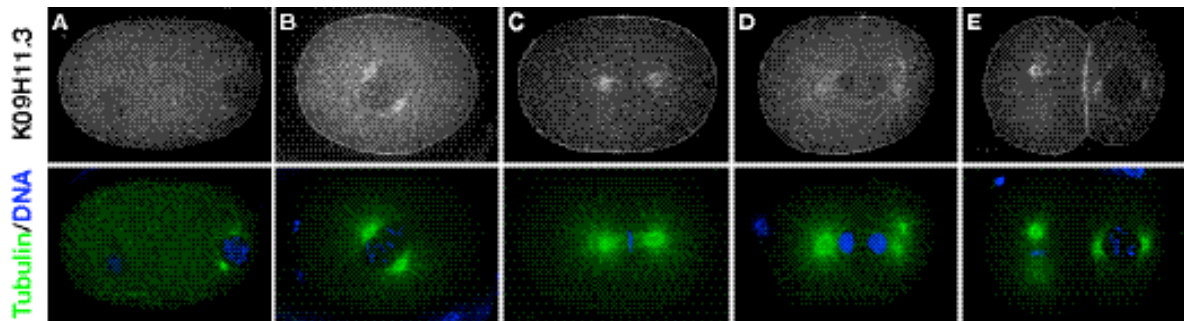
Figure 17. K09H11.3 localizes to both cortex and centrosomes

Embryos were stained for K09H11.3, microtubules (green) and for DNA (blue). K09H11.3 localizes to both cortex and centrosomes throughout the first cell cycle. (A) Pronuclear migration. (B) Pronuclear rotation. (C) Metaphase. (D) Late anaphase. (F) Two cell stage.
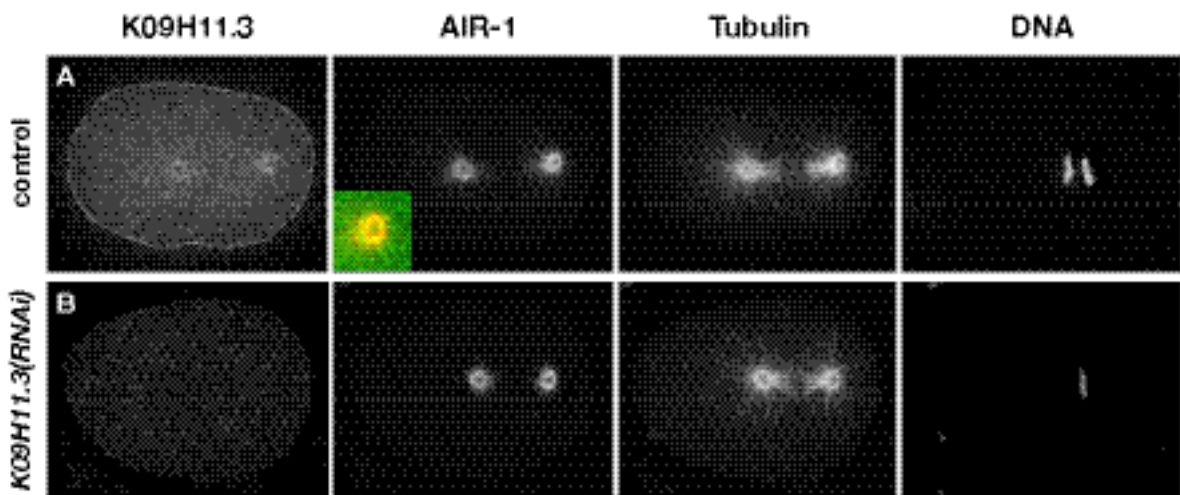
Figure 18. *K09H11.3(RNAi)*

Embryos were stained for K09H11.3, AIR-1, microtubules and for DNA. (A) Control embryo. Inset in second image left shows the overlay of K09H11.3 (green) and AIR-1 (red) localization (projection of 3 z-stacks, respectively) on the centrosome. K09H11.3 and AIR-1 partially overlap. (B) After *K09H11.3(RNAi)* K09H11.3 protein is not detectable.

2.4.3 Cortical K09H11.3 localization is independent of the centrosome

To examine whether the cortical localization of K09H11.3 is dependent on the formation of a functional centrosome, SPD-5 was depleted by RNAi and stained for K09H11.3 (Figure 19). SPD-5 is a protein required for the recruitment of pericentriolar material (PCM) (Hamill et al., 2002; Pelletier et al., 2004). Double labeling of embryos with K09H11.3 and SPD-5 revealed that K09H11.3 localizes around SPD-5, indicating that K09H11.3 is not a core centrosomal component; but rather a peripheral protein (Figure 19A, inset). After depletion of SPD-5, the K09H11.3 centrosomal localization is lost, but the cortical localization persisted, indicating that the cortical localization of K09H11.3 is independent of the centrosomal localization.
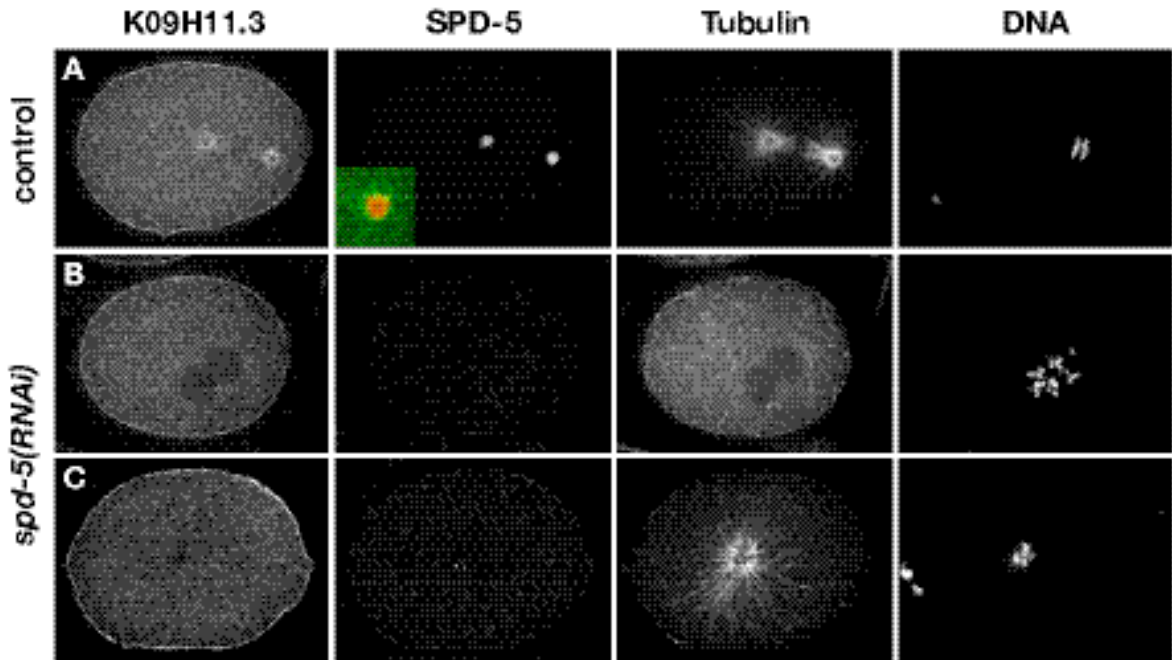
Figure 19. Cortical K09H11.3 localization is independent of the centrosome

Embryos were stained for K09H11.3, SPD-5, microtubules and for DNA. In (A) control embryos, K09H11.3 localizes to the centrosomes and on the cortex. Inset in second image left shows the overlay of K09H11.3 (green) and SPD-5 (red) localization (one single focal plane, respectively) on the centrosome. K09H11.3 localizes around SDP-5. In *spd-5(RNAi)* embryos at (B) pronuclear meeting and at (C) metaphase, the cortical localization of K09H11.3 was normal. (C) Residual SPD-5 is confined to two small dots. K09H11.3 is not detectable in the same region.

2.2.4 K09H11.3 is required for normal contractility, cytokinesis and polar body extrusion

To investigate the function of K09H11.3 in polarity establishment, K09H11.3 was depleted by RNAi. *K09H11.3(RNAi)* resulted in small and round embryos. The most pronounced defect in *K09H11.3(RNAi)* embryos was excessive anterior cortical contractility. In most of the embryos, incomplete cleavage furrow closure and the formation of cytoplasts occurred during cytokinesis, resulting in abnormal cellular arrangements (Figure 20C; Supplemental Movie S22). The next divisions often followed immediately or occurred synchronously with the first division and generated directly a four-cell embryo. The cleavage plane was often formed in the anterior half of the embryo and appeared to roam back and forward in the cell before it cleaved (Figure 20B). Additionally, *K09H11.3(RNAi)* embryos showed meiotic defects. After fertilization the zygote completes meiosis I and II and extrudes two polar bodies. In *K09H11.3(RNAi)* embryos, I often observed extra pronuclei in the anterior half. It seemed that these extra nuclei resulted from failure in polar body extrusion (data not shown). Sometimes these extra nuclei interfered with the spindle formation, leading to a tripolar spindle (Figure 20A). Given that both polar body extrusion and cytokinesis are mechanistically similar, suggests that the polar bodies are not extruded as a result of incomplete furrow closure as observed during cytokinesis in *K09H11.3(RNAi)* embryos.
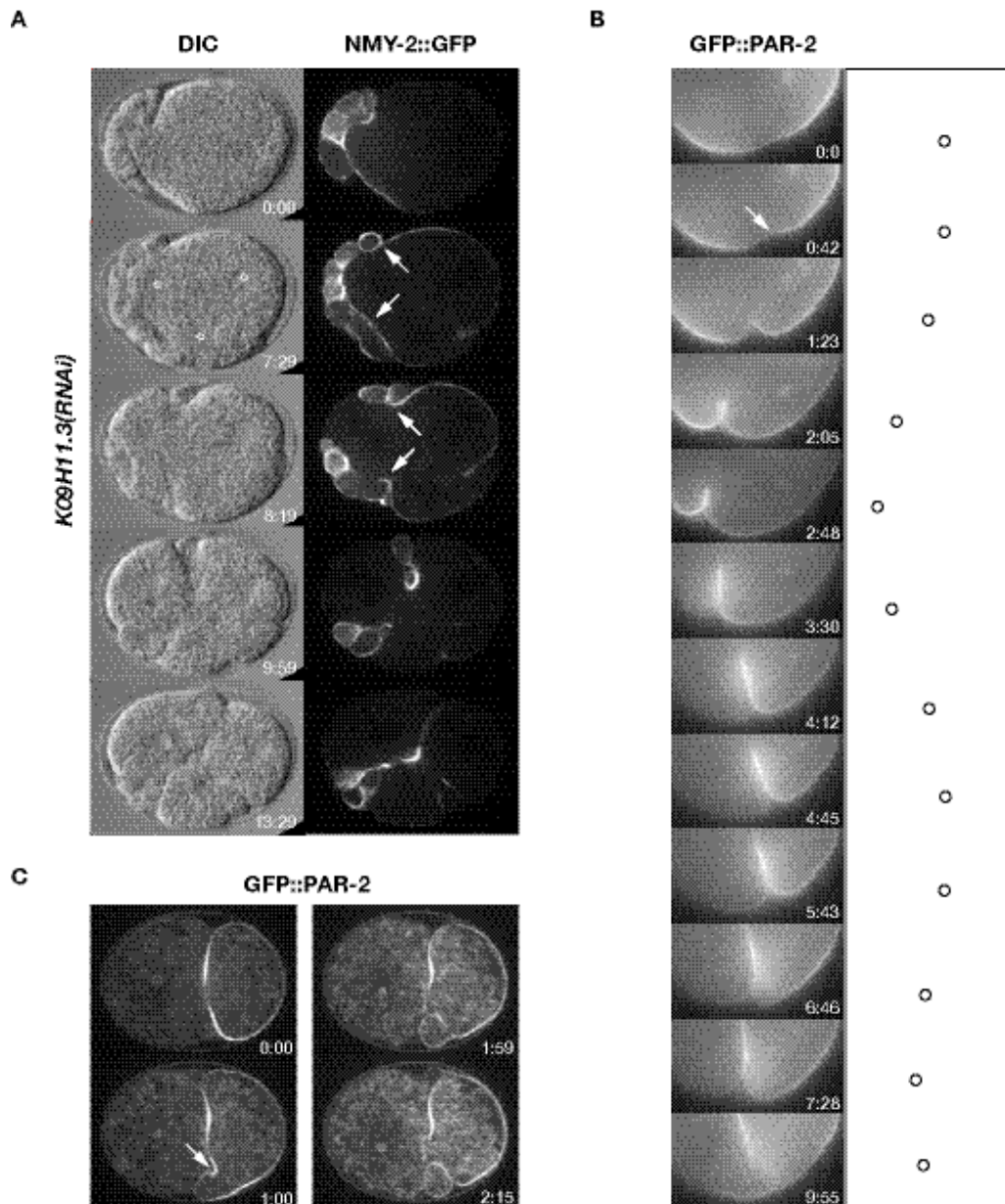
Figure 20. K09H11.3 is required for cytokinesis

Time-lapse images of (A) GFP::NMY-2 and (B, C) GFP::PAR-2 during cytokinesis. Times (min) are relative to the beginning of cleavage (A and B). (A) In most of *K09H11.3(RNAi)* embryos a new cleavage furrow is formed next to the persisting PSCF. In only 2 out of 24 embryos PSCF was moving back to the embryo center for cleavage. White stars mark the triple spindle. (B) Similar to the PSCF movement, the cleavage furrow often formed too far anterior in *K09H11.3(RNAi)* embryos. The furrow was moving back and forward until it cleaved asymmetrically (right). White arrow marks the initial position of cleavage furrow ingression. Black circles mark the position of the cleavage furrow over time (right). (C) In most of *K09H11.3(RNAi)* embryos cleavage was not completed. Cytoplast formed and the furrow reopened. White arrow marks the formation of a cytoplast.

52

2.2.5 K09H11.3 is required for the position of the boundary between the smooth and the contractile cortex

To investigate cortical dynamics in more detail, ruffle kymographs were generated and the position of the pseudocleavage furrow relative to the posterior pole was measured (Figure 21). In *K09H11.3(RNAi)* embryos, contractile polarity formed (Figure 21B), but the boundary between the smooth posterior and the anterior contractile cortex was shifted towards the anterior pole (Figure 21B and C), resulting in a large smooth and a small hypercontractile cortex. In control embryos, the pseudocleavage furrow moved about 50 ± 3% (n=15) of embryo length towards the anterior, whereas in *K09H11.3(RNAi)* embryos the pseudocleavage furrow moved 78 ± 7.5% (n=15) towards the anterior (Figure 21C). This indicates that K09H11.3 plays a role in pseudocleavage furrow positioning.

2.2.6 K09H11.3 is required to position the boundary between the anterior and posterior PAR proteins

To investigate whether increased cortical activity by *K09H11.3(RNAi)* modulates formation of PAR domains, time-lapse recordings of GFP::PAR-2 and GFP::PAR-6 were made. GFP::PAR-2 localization was normal during meiosis in *K09H11.3(RNAi)* embryos (Figure 22), but the GFP::PAR-2 domain size during embryo polarization was larger than in control embryos (Figure 23A; Supplemental Movie S23). In control embryos, the extension of the GFP::PAR-2 domain appears to coincide with movement of the pseudocleavage furrow. To investigate whether GFP::PAR-2 domain follows the movement of the pseudocleavage furrow, the position of the pseudocleavage furrow together with the position of GFP::PAR-2 domain boundary were tracked over time (Figure 24). The analysis revealed that, similar to control embryos, after *K09H11.3(RNAi)* both positions coincide. The calculation of the maximal extent of the GFP::PAR-2 domain as a fraction of the embryo circumference revealed that the maximal size of the GFP::PAR-2 domain was greater in *K09H11.3(RNAi)* embryos (67 ± 4 %) than in control embryos (53 ± 2 %) (Figure 23). Similar to control embryos, GFP::PAR-6 segregated to the anterior and was confined to the contractile cortex. GFP::PAR-6 localized to the cortical ingressions (Figure 25B; Supplemental Movie S24). These results suggest that the PAR domains respond to the change of cortical contractions. K09H11.3 is required for positioning of the boundary between contractile and non-contractile cortex and the anterior and posterior PAR domains.
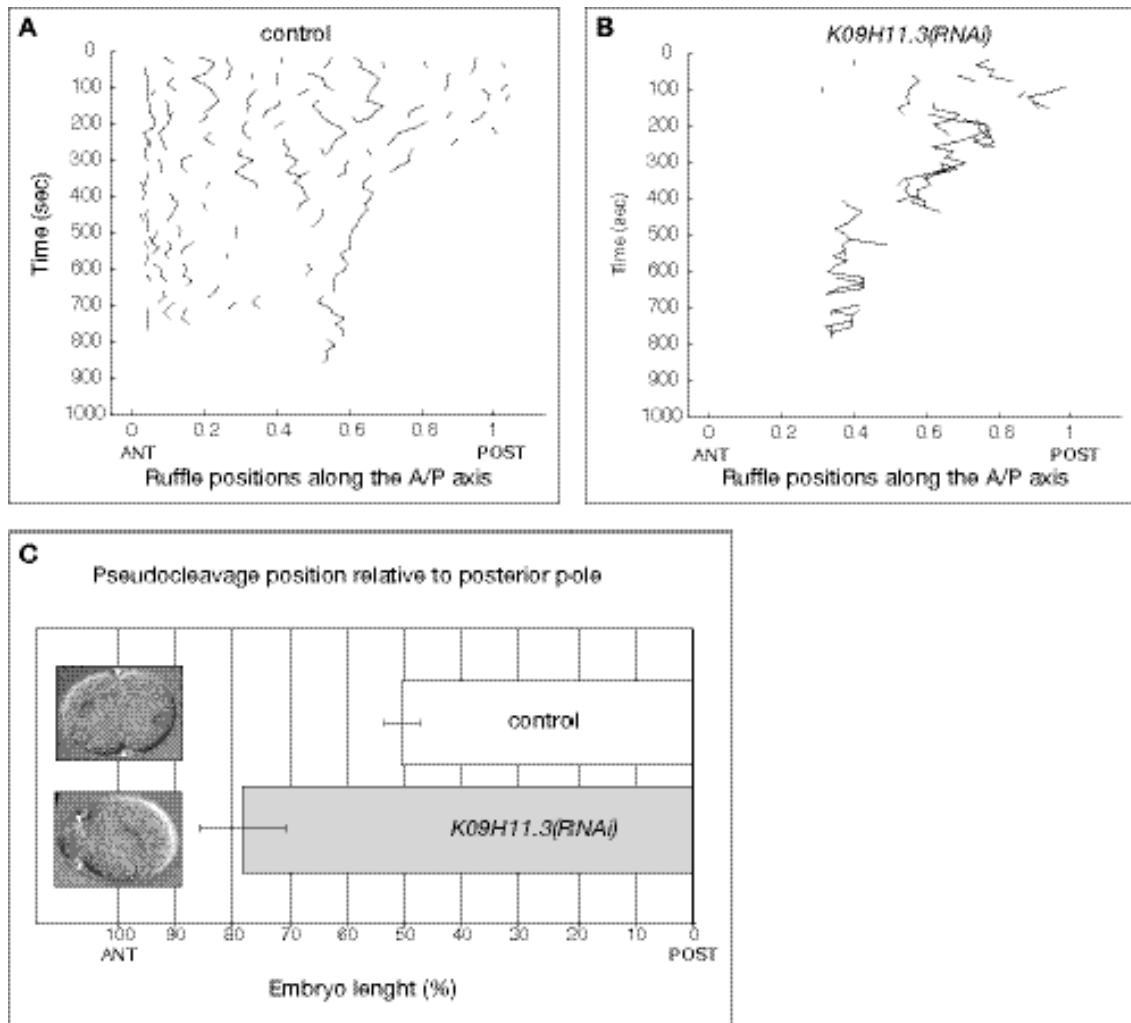
Figure 21. K09H11.3 is required to position the pseudocleavage furrow

(A, B) Ruffle kymographs monitoring the establishment of contractile polarity over time.

(A) In control embryos the cortex contracts uniformly after completion of meiosis. During anterior-posterior polarity establishment, the posterior cortex becomes cleared from contractions, while the anterior cortex continuous to ruffle. (B) In *K09H11.3(RNAi)* embryos the contractile polarity was established; however, the ruffles were deeper and persisted longer and cytoplasts were formed. The pseudocleavage furrow (PSCF) moved more anterior than in control embryos. In *K09H11.3(RNAi)* embryos the ruffles were only tracked for a period of 800 seconds. (C) Position of PSCF relative to posterior pole. In control embryos, PSCF moves 50 ± 3% (n=15), in *K09H11.3(RNAi)* embryos, PSCF moves 78 ± 7.5% (n=15) of embryo length away from the posterior pole.

54
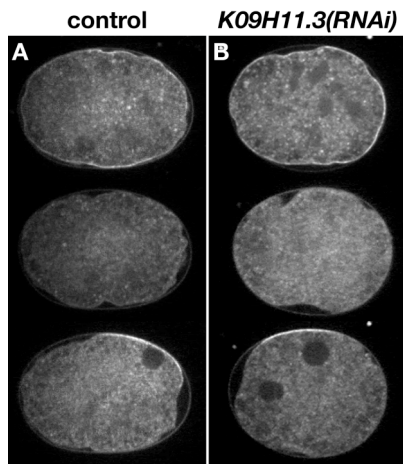
Figure 22. Meiotic PAR-2 cycle is normal in _K09H11.3(RNAi)_ embryos

Time-lapse images of GFP::PAR-2 polarity establishment in (A) control and (B) _K09H11.3(RNAi)_ embryos. (A) In control embryos, GFP::PAR-2 localizes uniformly along the cortex around the time of meiosis (top). After meiosis GFP::PAR-2 disappears from the cortex (middle) and then becomes confined to the posterior pole (bottom). (B) In _K09H11.3(RNAi)_ embryos the GFP::PAR-2 cycle is not impaired.
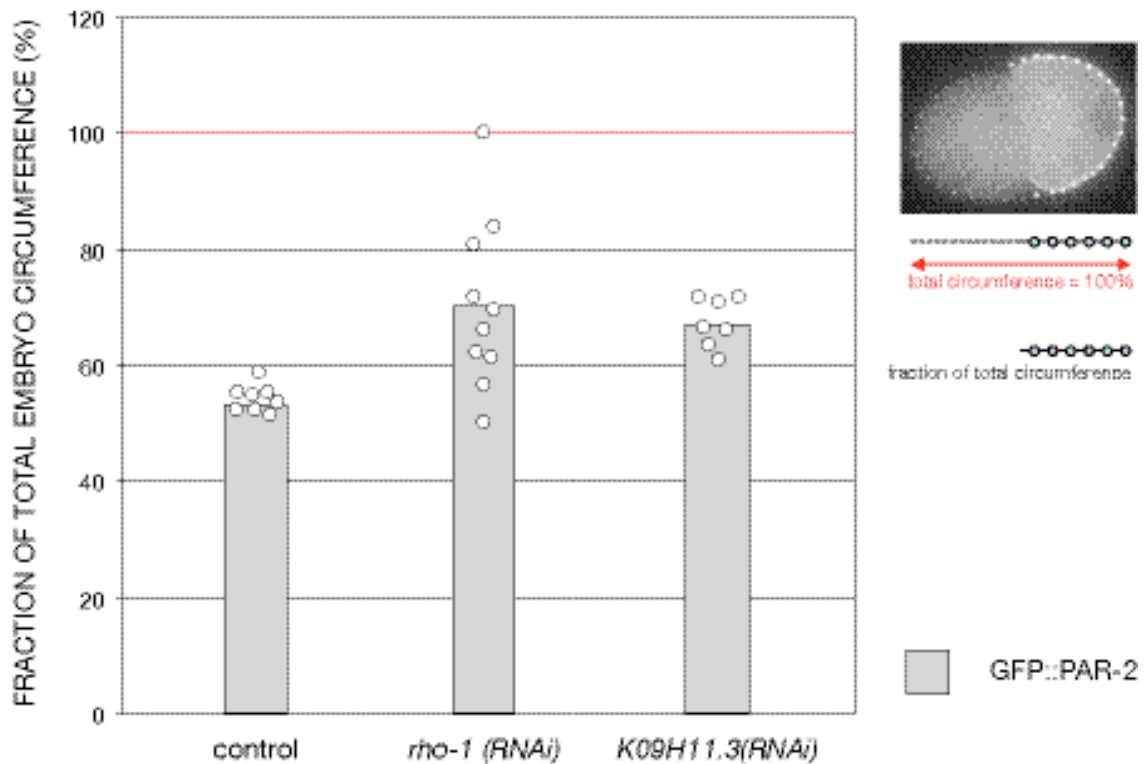
Figure 23. K09H11.3 is involved in regulating the PAR-2 domain size

The GFP::PAR-2 domain size was manually tracked after the GFP::PAR-2 domain reached its maximal extent. The domain size was calculated as a fraction of the embryo circumference. In control embryos, the GFP::PAR-2 domain extent amounts to 53 ± 2% (n=8). In *rho-1(RNAi)* embryos, GFP::PAR-2 domain extent amounts to 70 ± 15% (n=10), whereas in *K09H11.3(RNAi)* embryos the extent was 67 ± 4% (n=7).
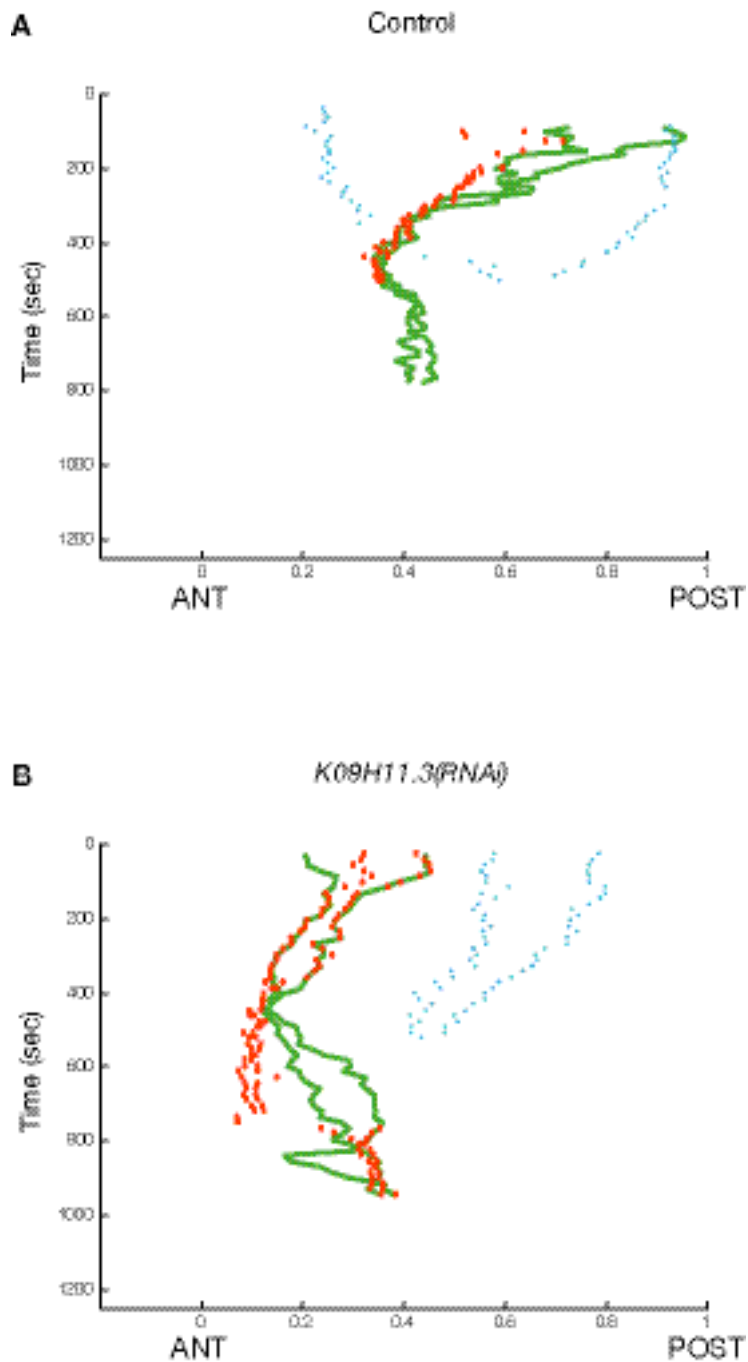
Figure 24. Kymographs of GFP::PAR-2 domain expansion and pseudocleavage furrow movement along the anterior-posterior axis

In both (A) control embryos and (B) *K09H11.3(RNAi)* embryos, the position of the GFP::PAR-2 domain boundaries (solid green lines) coincides with pseudocleavage furrow position (red dots). Around cytokinesis PAR-2 retracts before the pseudocleavage furrow in *K09H11.3(RNAi)* embryos. Position of pronuclei is marked by blue dots.

57
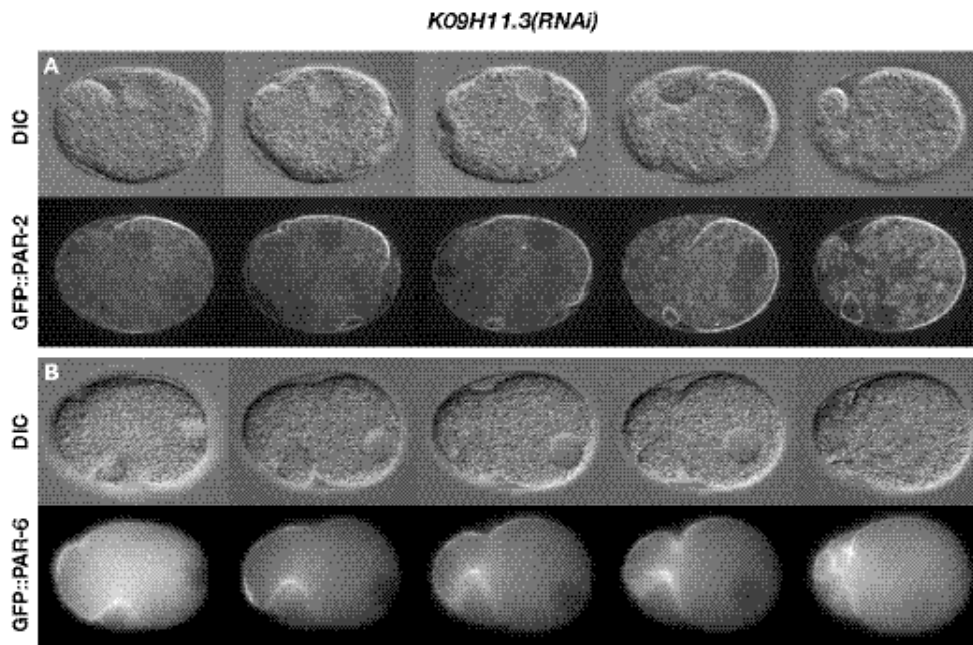
K09H11.3(RNAi)

Figure 25. K09H11.3 is required to restrict PAR-2 to the posterior half

Time-lapse images of (A) GFP::PAR-2 and (B) GFP::PAR-6 during polarity establishment in *K09H11.3(RNAi)* embryos. (A) GFP::PAR-2 domain follows the PSCF movement. Both move too far anteriorly. (B) GFP::PAR-6 is confined to the contractile cortex.

2.2.7 *K09H11.3(RNAi)* alters the organization and dynamics of NMY-2

To analyze the contractile activity in *K09H11.3(RNAi)* embryos in more detail, NMY-2::GFP was used to monitor myosin organization and dynamics. Cortical views showed that NMY-2::GFP segregated to the anterior in *K09H11.3(RNAi)* embryos, but the structure of the NMY-2-GFP meshwork appeared different than in control embryos. In *K09H11.3(RNAi)* embryos, dense NMY-2 filaments were formed, which appeared to be enriched in cortical invaginations (Figure 26). This suggests that K09H11.3 is implicated in the organization of the NMY-2 meshwork.
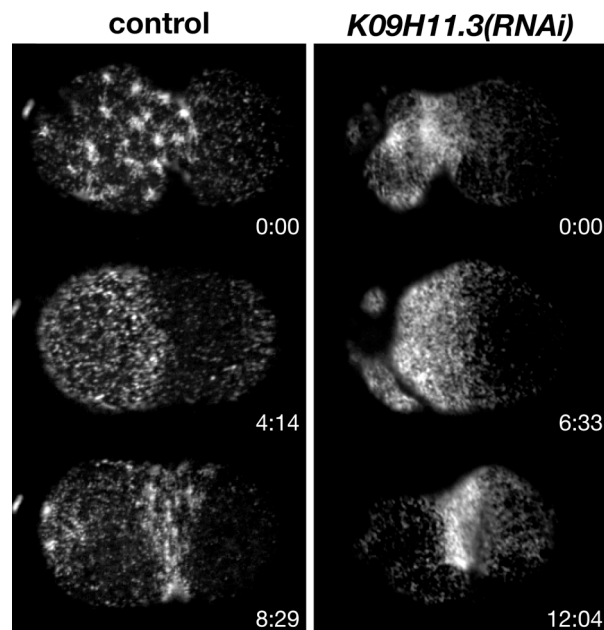
Figure 26. *K09H11.3(RNAi)* alters NMY-2 organization

Time-lapse images (surface view) of GFP::NMY-2 during polarity establishment of control (left) and *K09H11.3(RNAi)* (right) embryos. Times are in min.

2.2.8 K09H11.3 is putative GAP for RHO-1, but not for CDC-42

To determine whether K09H11.3 is a GAP for RHO-1 or for CDC-42 or for both, K09H11.3 was simultaneously depleted with RHO-1 or CDC-42, and GFP::PAR-2 and GFP::PAR-6 localization was analyzed (Figure 27). *K09H11.3(RNAi);rho-1(RNAi)* resulted in loss of contractile activity and GFP::PAR-2 and GFP::PAR-6 showed localization defects as in *rho-1(RNAi)* embryos (Supplemental Movies S25 and S26). The fact that this double mutant phenotype resembled *rho-1(RNAi)*, suggested that K09H11.3 regulates RHO-1. In contrast, double depletion of K09H11.3 and CDC-42 resulted in high cortical activity in the anterior cortex, similar to what was observed for *K09H11.3(RNAi)* alone. Furthermore, GFP::PAR-2 and GFP::PAR-6 in *K09H11.3(RNAi);cdc-42(RNAi)* embryos localized as after *K09H11.3(RNAi)* (Supplemental Movies S27 and S28). This indicates that CDC-42 is not regulated by K09H11.3. However, to confirm the specificity of K09H11.3 for RHO-1 detailed biochemical assays would be required.
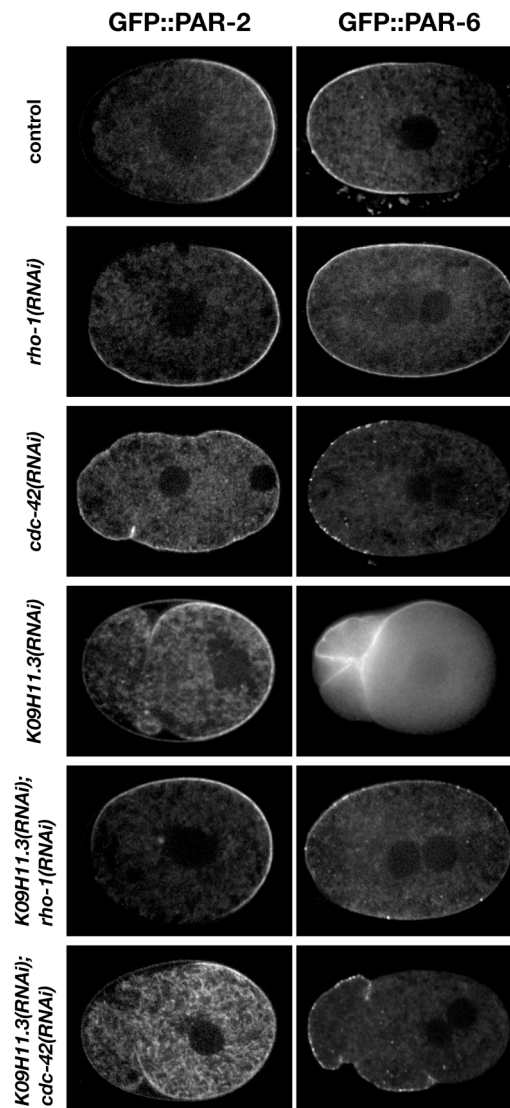
Figure 27. K09H11.3 acts on RHO-1

Images of GFP::PAR-2 (left) and GFP::PAR-6 (right). *K09H11.3(RNAi);rho-1(RNAi)* embryos display the *rho-1(RNAi)* phenotype, whereas *K09H11.3(RNAi);cdc-42(RNAi)* embryos display the *K09H11.3(RNAi)* phenotype, indicating that K09H11.3 acts as a GAP only on RHO-1.

3. DISCUSSION

In the *C. elegans* embryo several studies have shown that the acto-myosin cytoskeleton is required for the establishment of PAR polarity (Cuenca et al., 2003; Guo and Kemphues, 1996b; Hill and Strome, 1988; Hill and Strome, 1990; Severson et al., 2002; Shelton et al., 1999), but how it contributes has been unclear. To investigate in more detail how the acto-myosin activity is required for polarity formation, the Rho GTPases family members RHO-1 and CDC-42 were used to modulate the acto-myosin dynamics. Since the control of Rho GTPase activity is critical for their spatial and temporal function, the roles of two uncharacterized potential regulators, the RhoGEF ECT-2 and the RhoGAP K09H11.3, were analyzed with respect to contractile and PAR polarity.

This study demonstrates that both RHO-1 and CDC-42 are involved in polarity establishment in *C. elegans* embryos. But importantly, they act by different mechanisms. RHO-1 organizes the acto-myosin cytoskeleton into a contractile network, and is therefore essential for the contractile polarity. Furthermore, it appears that the organization of the acto-myosin cytoskeleton is critical to ensure proper PAR protein distribution. The balance of RHO-1 activity as regulated by the GEF ECT-2 and the GAP K09H11.3 seems to be important for the PAR protein domain size and for their mutual exclusion. Furthermore, RHO-1 activity is required for localizing CDC-42. In contrast, CDC-42 appears to act downstream of contractile polarity, but upstream of PAR protein polarity, and is required for PAR localization, possibly by linking PAR-6 to the cortex.

3.1 CDC-42 acts upstream of the PAR proteins

3.1.1 CDC-42 is involved in the meiotic PAR-2 cycle

Previous studies with fixed samples have indicated CDC-42 involvement in *C. elegans* polarity formation (Gotta et al., 2001; Kay and Hunter, 2001). From these analyses, it was concluded that CDC-42 primarily plays a role in polarity maintenance, whereas the present investigation proposes that CDC-42 is required for early PAR protein localization. By using time-lapse imaging of GFP::PAR-2, this analysis shows that PAR-2 localization undergoes a cycle and that this cycle is impaired in the absence of CDC-42. In *cdc-42(RNAi)* embryos, PAR-2 does not disappear from the cortex after meiosis II. In *cdc-42(RNAi);spd-2(RNAi)* embryos lacking the polarizing cue (SPD-2), PAR-2 localized uniformly to the cortex, suggesting that cortical PAR-2 localization in *cdc-42(RNAi)*

embryos is independent of the embryo polarization. Thus, these experiments demonstrate that meiotic PAR-2 localization does not depend on the centrosome, and furthermore, that CDC-42 has a role in removing PAR-2 from the cortex during meiosis II.

3.1.2 CDC-42 is required to effectively link PAR-6 to the cortex

How could CDC-42 be involved in the meiotic PAR-2 cycle? CDC-42 localization was normal in the absence of either PAR-3 or PAR-6, indicating that CDC-42 acts upstream of the anterior PAR proteins. Given that CDC-42 interacts with PAR-6 (Gotta et al., 2001; Hutterer et al., 2004; Joberty et al., 2000; Johansson et al., 2000; Lin et al., 2000; Qiu et al., 2000) and that *cdc-42(RNAi)* prevented PAR-6 localization to the cortex, the uniform localization of PAR-2 in *cdc-42(RNAi)* embryos may be a direct consequence of the failure to localize PAR-6 to the cortex at the end of meiosis. Consistent with this idea, PAR-2 is uniformly localized in *par-6* mutants (Cuenca et al., 2003; Watts et al., 1996).

3.2 Contractile polarity is upstream of CDC-42

In *cdc-42(RNAi)* embryos, PAR polarity was disrupted although contractile polarity was formed. Given that RNAi is a run-down technique, it cannot be excluded that a complete loss of CDC-42 function would abolish contractile polarity. In support of the finding that CDC-42 does not play a major role in contractile polarity formation, depletion of a putative downstream effector of CDC-42, Arp2/3, does not affect cortical ruffling (Severson et al., 2002). Nevertheless, CDC-42 is somehow involved in cortical dynamics in the embryo. The finding that in *cdc-42(RNAi)* embryos the anterior localization of NMY-2 was transient suggests that CDC-42 is somehow implemented in stabilizing the acto-myosin network at the anterior cortex.

3.3 RHO-1 links the establishment of contractile polarity to the establishment of PAR polarity

Depletion of either RHO-1 or ECT-2 abolished contractile polarity. Further analysis showed that ECT-2 is most likely a GEF for RHO-1 since it displayed an identical phenotype to RHO-1. Studies with NMY-2::GFP showed that in *rho-1(RNAi)* and *ect-2(RNAi)* embryos, the organization of NMY-2 into a dynamic contractile network is abolished. This suggests that RHO-1 activity is essential for the assembly of the contractile network, which in turn is responsible for the formation of the contractile polarity. In wild type embryos, NMY-2::GFP forms a dynamic network throughout the

entire cortex. The network disassembles in the vicinity of the posterior nucleus/centrosome complex and begins to segregate towards the anterior. It was suggested that anterior PAR proteins are carried by this movement, since GFP::PAR-6 and NMY-2::GFP moved at the same velocity to the anterior cortex (Hird and White, 1993; Munro et al., 2004). In *rho-1(RNAi)* and *ect-2(RNAi)* embryos, although the acto-myosin structure was defective, the NMY-2 cytoskeleton was still able to segregate. However, PAR-6 was always uniformly distributed throughout the first cell cycle, showing that in *rho-1(RNAi)* and *ect-2(RNAi)* embryos, NMY-2::GFP segregation is uncoupled from GFP::PAR-6's anterior migration. Thus, the function of RHO-1 may be to couple the segregation of the acto-myosin cytoskeleton to the segregation of the anterior PAR complex by organizing the cytoskeleton into a contractile network.

3.4 RHO-1 localizes CDC-42 to the anterior cortex

CDC-42 localized to the cortex in the absence of RHO activity (*ect-2(RNAi)*), however the segregation of CDC-42 to the anterior cortex did not occur. This suggests that RHO-1, by organizing the actin-myosin cytoskeleton into a contractile network, regulates the segregation of CDC-42 to the anterior. CDC-42 may provide the link between PAR-6 and the cortex, thereby linking the segregation of the anterior PAR complex to segregation of the actin-myosin cytoskeleton. ECT-2 was shown to interact with PAR-6 in epithelial cells (Liu et al., 2004). This interaction may help to stabilize the interaction of CDC-42 and the anterior PAR complex with the cortex. So far, it is still unclear what recruits and activates CDC-42 at the cortex and whether CDC-42 GTPase activity is required for its role in polarity establishment. One putative candidate for CDC-42 activation could be a homolog of the yeast RhoGEF CDC-24, which was shown to bind to the bud scar and activate CDC-42 in yeast (Johnson, 1999). A clear homolog of CDC-24 is not evident in the *C. elegans* genome.

3.5 RHO-1 activity controls the boundary between PAR-2 and PAR-6

In control embryos, the localization of the anterior and the posterior proteins is mutually exclusive. However, in *rho-1(RNAi)* and *ect-2(RNAi)* embryos, PAR-2 was observed to overlap with PAR-6. This suggests that RHO-1 might function through the cytoskeleton to establish the boundary between anterior and posterior PAR proteins. Furthermore, in those embryos in which GFP::PAR-2 appeared at the cortex, the PAR-2 domain was spreading along the cortex and in extreme cases, PAR-2 was uniformly distributed in the

end. This shows that RHO-1 activity is implicated in the regulation of PAR-2 domain size, but it is not quite clear how RHO-1 could accomplish this. This feature appears only in *rho-1(RNAi)* embryos. Depletion of proteins implicated in regulation or formation of the acto-myosin cytoskeleton does not result in spreading of PAR-2 (Cuenca et al., 2003; Guo and Kemphues, 1996b; Hill and Strome, 1990; Severson et al., 2002; Severson and Bowerman, 2003; Shelton et al., 1999). The analysis of a strain expressing both NMY-2::GFP and GFP::PAR-2 showed that the movement of both proteins correlates in control as well as in *rho-1(RNAi)* or *ect-2(RNAi)* embryos. Therefore, RHO-1 could regulate the size of the PAR-2 domain via the regulation of the acto-myosin network. One model of how cortical polarity is established suggests that the cortical acto-myosin meshwork is under tension and that a local break in the meshwork causes the meshwork to collapse away from the break-point (Hird and White, 1993), leaving the voided region of the cortex available for PAR-2 localization. RHO-1 could modulate the contractile forces within the network, which could result in an alteration of the boundary between the cytoskeletal network and the PAR-2 domain.

Different amounts of GFP::PAR-2 at the cortex are likely to result from partial RHO-1 depletion, which proposes that complete loss of RHO-1 function is reflected by the absence of GFP::PAR-2. However, it is questionable whether complete loss of RHO-1 function in the embryo is possible to obtain, since RHO-1 also seems to be implicated in the formation of oocytes. Oocytes are formed by pinching off from the proximal arm of the gonad, a process similar to cytokinesis in which RHO-1 is involved. In *rho-1(RNAi)* worms, the gonad was long and unsegmented (data not shown) and it was difficult to obtain embryos from these worms, indicating that some RHO-1 activity is required for embryo formation. Therefore, it is likely that the analyzed embryos in which PAR-2 was spreading along the cortex contained residual RHO-1 activity.

3.6 Cytoplasmic flows occur with PAR-2 appearance

The occurrence of cytoplasmic flows correlates with the establishment of polarity. It has been shown that the acto-myosin cytoskeleton is required to create these flows. The observation that yolk granules, NMY-2::GFP foci and GFP::PAR-6 puncta move with similar speed away from the posterior pole suggested that the cytoskeleton transports proteins, including the PAR-3/Par-6/PKC-3 complex, to the anterior (Munro et al., 2004). Since in *rho-1(RNAi)* or *ect-2(RNAi)* embryos contractile polarity is abolished and the GFP::PAR-6 does not segregate, cytoplasmic flows were analyzed. Although apparent

cortical contractility was absent in *ect-2(RNAi)* and *rho-1(RNAi)* embryos, cytoplasmic flows occurred when PAR-2::GFP was present at the cortex as in control embryos. This confirms previous suggestions that establishment of a cortical GFP::PAR-2 domain is linked with the appearance of cytoplasmic flows (Cheeks et al., 2004), but appears contradictory to the idea that contractility is required for creating cytoplasmic flows. One explanation could be that small amounts of residual RHO-1 activity are somehow capable of creating these flows, or that different levels of acto-myosin activity are required for contractility and cytoplasmic flows.

3.7 K09H11.3 alters cortical contractility

The regulation of Rho GTPase activity requires the balanced action of RhoGEFs and RhoGAPs. Inactivation of a GAP leads to constitutively active GTPase and allows the study of active Rho GTPase in the cell. Depletion of K09H11.3 resulted in a very complex phenotype because several processes in the embryo appeared to be affected. The most prominent phenotype was exaggerated cortical activity restricted to the anterior embryo half. Tracking of the cortical ingressions over time revealed that contractile polarity formed, but that the boundary between contractile and non-contractile cortex, the pseudocleavage furrow, moved too far anterior, indicating that K09H11.3 is involved in positioning the pseudocleavage furrow. Given that the establishment of contractile polarity is a consequence of the anterior segregation of the actin cytoskeleton, the hypercontractility might be a manifestation of an increase of intrinsic contractions of the cytoskeleton towards the anterior pole. It is hypothesized that the cortical meshwork is under tension and that a local weakening of the network by a signal from the centrosome is sufficient to cause the network to collapse and to contract towards the opposite pole (Hird and White, 1993). It is therefore possible that *K09H11.3(RNAi)* increases the disassembly at the posterior cortex, which causes the cytoskeleton to segregate too far anterior. The analysis of the NMY-2::GFP meshwork in *K09H11.3(RNAi)* embryos could show enrichment and an increase of filamentous NMY-2::GFP in the anterior contractile half, but it was difficult to determine whether the acto-myosin network was more condensed.

3.8 Local restriction of K09H11.3 activity

How could K09H11.3 activity cause local disassembly of the cytoskeleton? The uniform distribution of K09H11.3 at the cortex does not help to determine how this may be

accomplished. Data about where in the embryo the protein is active is missing. It is possible that although the protein is uniformly distributed along the cortex, it is active only in specific regions. The regulation of Rho GAP activity involves posttranslational modifications. For example, phosphorylation of the RhoGAP p190RhoGAP by Src is necessary for its association with p120Ras GAP and activation of its GAP activity (Roof et al., 1998). More recently it was shown that MgcRacGAP (homolog of the *C. elegans* protein CYK-4) involved in cytokinesis, is functionally converted into a GAP for RhoA after phosphorylation by Aurora B kinase (Minoshima et al., 2003). Other Rho GAPs have also been shown to be regulated by lipid interaction, protein-protein interaction and proteolytic degradation (Ahmed et al., 1993; Jenna et al., 2002). Therefore, it could be possible that K09H11.3 activity is restricted to the posterior half. Local activation of the GAP in the posterior could lead to local inactivation of RHO-1 activity, which in turn disassembles the acto-myosin filaments at the posterior cortex. Since the network is under tension, a local disassembly would lead automatically to segregation of the cytoskeleton towards the anterior pole.

3.9 K09H11.3 centrosomal location

A clue to how K09H11.3 might locally control contractility came from the finding that K09H11.3 localizes to the centrosomes as well as the cortex. Double labeling with SPD-5 or AIR-1 revealed that K09H11.3 localizes in a donut-shaped region around SPD-5 and partially overlaps with AIR-1 localization. The function of K09H11.3 on the centrosome remains to be elucidated, but K09H11.3 could be a phosphorylation target of AIR-1, which also displays a polarity phenotype after depletion by RNAi.

Preliminary results show that after depletion of the centrosomal protein SPD-5 only the centrosomal localization of K09H11.3 was abolished. This result will allow to determine whether the localization of K09H11.3 is implicated in polarity formation or other processes by performing *spd-5(RNAi);K09H11.3(RNAi)*. In particular, it will be interesting to study whether the centrosomal localization of K09H11.3 is important for polarity formation and the contractile activity of the cortex. Depletion of the centrosomal protein SPD-5 was shown to abolish segregation of the NMY-2::GFP (Munro et al., 2004). However, how the signal from the centrosome is transmitted to the molecular target at the cortex is still unknown. Activation of a GAP localized on the centrosome and the cortex, might act as transmitter. K09H11.3 could be a potential candidate.

3.10 K09H11.3 a GAP for RHO-1?

Whether K09H11.3 acts as a GAP on RHO-1 is still not clear. Although double depletion of K09H11.3 with RHO-1 or CDC-42 suggested that the GAP is more likely to act on RHO-1 than on CDC-42, the phenotype of *K09H11.3(RNAi)* does not give information whether the K09H11.3 is acting as a GAP for RHO-1. Since *rho-1(RNAi)* abolishes all aspects of contractility one would expect that constant active RHO-1 signaling would induce hypercontractility throughout the cortex. In *K09H11.3(RNAi)* embryos contractile polarity is formed and the hypercontractility is confined to the anterior, which raises the question whether the protein is only partially depleted or whether this is the full loss-of-function phenotype. Unfortunately, the mother worms appear to become sterile since the number of embryos decreased with longer RNAi incubation and made it difficult to push the RNAi conditions to the limit. Another explanation could be that another Rho GAP is involved in cortical contractility. So far, only the Rho GAP CYK-4 was identified to play a role in the one-cell embryo. CYK-4 was shown to act as GAP for RHO-1 in cytokinesis (Jantsch-Plunger et al., 2000), but its role in polarity formation is not known. It is also possible that after *K09H11.3(RNAi)*, its paralog Y75BAL.4 is still active and partially compensates for the loss of K09H11.3. The proteins share about 79 % protein similarity. Although RNAi using a small RNA specific to Y75B7AL.4 resulted in no phenotype, the possibility cannot be ruled out that this RNA was not functional. Therefore, the establishment of contractile polarity in *K09H11.3(RNAi)* embryos could be explained by the presence of Y75B7AL.4, although it appears unlikely. Another explanation could be that K09H11.3 does not regulate the activity of Rho. It is known that GAP proteins, apart from being negative regulators, can solely function as downstream effectors of Rho GTPases. For instance, n-chimaerin can induce actin reorganization independently of its Rho GAP domain (Kozma et al., 1996).

3.11 Model

On the bases of this data and from data of other publications, the following model how anterior-posterior polarity could form can be proposed: The Rho GEF ECT-2 activates and localizes RHO-1 at the cortex prior to polarity establishment. Cortical localized RHO-1 organizes actin and myosin into a contractile network by regulating actin polymerization and myosin activity. The ruffling might be a manifestation of the assembly of the contractile network. The assembly of actin and myosin into a contractile network

allows localization and/or activation of CDC-42 at the cortex, where it triggers assembly of the anterior PAR complex. A signal from the centrosome, which could be transmitted by a Rho GAP to the cortex, leads to local inactivation of RHO-1 at the posterior cortex causing the disassembly and segregation of the actin-myosin cytoskeleton. The cytoskeleton carries the CDC-42/PAR-3/PAR-6/aPKC complex away from the posterior pole, leaving a region available for PAR-2 localization.

4. MATERIAL AND METHODS

Worm strains

Worms were handled as described (Brenner, 1974). The following strains were used: N2 (wild type), JH1380 (GFP::PAR-2), TH25 (GFP::PAR-6), JJ1473 (NMY-2::GFP), TH71 (NMY-2::GFP;GFP::PAR-2), TH72 (YFP::CDC-42).The TH71 strain was constructed by crossing JH1380 to JJ1473 and progeny were selected that expressed both GFPs. The N-terminal YFP-tagged CDC-42 is expressed under the *pie-1* promoter (TH72). Microparticle bombardment (BioRad) was used to generate transgenic worms, as described previously (Praitis et al., 2001).

RNA-mediated interference

RNAi experiments were performed as described (Oegema et al., 2001). Primers used to amplify regions from N2 genomic DNA are listed in Table 1 (without T3 and T7 RNA polymerase promoter tails). The PCR products were purified by using a PCR clean up kit (Qiagen), eluted with 40 µl water and used as templates for 25 µl T3 and T7 transcription reactions (Ambion). After incubating the transcription reactions for 3-5 hours at 37 °C, DNase (1.3 µl/reaction) was added and incubated for 15 min at 37 °C. The reactions were cleaned using an RNeasy kit (Qiagen), and the RNA was eluted in a final volume of 60 µl. T3 and T7 reactions were pooled and mixed with 3x injection buffer (60 mM KPO_4 pH 7.5, 9 mM K-Citrate pH 7.5 and 6% PEG 6000). Annealing was performed by incubating the reaction at 94 °C for 10 min, followed by an incubation of 1 hour at 37 °C. Samples form T3 and T7 transcription reactions and a sample of the annealed double-stranded (ds) RNA was loaded on a gel. Annealed dsRNA exhibited a band shift compared to single-stranded RNAs. DsRNA was aliquoted, snap-frozen in liquid nitrogen and stored at –80 °C.

The dsRNA was injected into L4 hermaphrodites and the worms were incubated depending on the individual double-stranded RNA for 10-22 hours at 25°C after injection. *Cdc-42(RNAi);rho-1(RNAi)* was performed by coinjection of both RNAs combined with the feeding of (*cdc-42(RNAi)* (Timmons and Fire, 1998). *Cdc-42(RNAi);spd-2(RNAi)* was performed by coinjection of both RNAs combined with feeding of *cdc-42(RNAi)* and *spd-2(RNAi)*. Worms were placed on feeding plates after injection and maintained at 25°C for 22 hours.

Table 1. Primers used to amplify regions from N2 genomic DNA for the production of double-stranded RNA *in vitro*. For RHO-1 depletion, a mixture of two short RNAs targeting two different regions of the gene was used.

	gene	forward	reverse
rho-1	Y51H4A.3	ATCGTCTGCGTCCACTCTCT	GGCTCCTGTTTCATTTTTGC
rho-1	Y51H4A.3	AAAACTTGCCTGCTCATCGT	TTCCGTCAACTTCAATGTCG
cdc-42	R07G3.1	TCAAAGACCCCATTCTTGTT	ACTTCTCTCCAACATCCGTT
ect-2	T19E10.1	TGGATCCGATTCTCGAACTT	ACATTTGGCTTTGTGCTTCC
K09H11.3	K09H11.3	CAAGTTGACGGACATATGCT	GAATTAATGGGTCTTGGTGA
K09H11.3	K09H11.3	CTGAGGTCTGCAACTGATGA	AAGTGCTCGATTTCCTGAAA
Y75B7AL.4	Y75B7AL.4	GAGGTTTGTGCTGCTGC	GCATACCATTTTCAGTGGAA
	K09/ Y75*	GGCATGAGCAGTGGATACGAA	GTCCTTCCTGAGCACGACTTT
spd-2	F32H2.3	AATGGTGGTCGCTTCAAAAC	TGACGGTAGAGACGGATGTG
spd-5	F56A3.4	TGTCGCAACCAGTTCTGAAT	ATGGAGGCAAATTGTTGCTG
par-3	F54E7.3	GTGACCGGACGTGAAACTG	TTTTCCTTCCGAGACCTTCC
par-6	T26E3.3	ATGTCCTACAACGGCTCCTA	TCAGTCCTCTCCACTGTCCG
mlc-4	C56G7.1	CTCCCGCAAAACCGTAAAC	TCATCCTTGTCCTTGGTTCC
pfn-1	Y18D10A.20	CTCCTCCAAAACACAAAAATGTC	AGAGAAAAGCGGGAATAAATAG

* Primers for RNA covering both K09H11.3 and Y75B7AL.4.

Worms were incubated depending on the individual double-stranded RNA for 10-22 hours at 25°C after injection. The incubation time was depending on the GFP-strain that was used. The incubation times listed below were used for GFP::PAR-2 and GFP::PAR-6 strain. The incubation times for NMY-2::GFP were in general 2-3 hours shorter.

Table 2. RNAi incubation times (25 °C)

	gene	incubation time		gene	incubation time
rho-1	Y51H4A.3	22h	mlc-4	C56G7.1	22h
rho-1	Y51H4A.3	22H	spd-2	F32H2.3	22h
cdc-42	R07G3.1	22h	spd-5	F56A3.4	22h
ect-2	T19E10.1	10h	par-3	F54E7.3	20h
K09H11.3	K09H11.3	22h	par-6	T26E3.3	20h
pfn-1	Y18D10A.20	20h		K09/ Y75*	22h

Time-lapse microscopy

Worms were shifted to 25°C before recording. Embryos were dissected and mounted in a solution containing 0.1 M NaCl and 4% sucrose, with and without 2% agarose. GFP, YFP and differential interference contrast (DIC) recordings were acquired at 10-15 second intervals (exposure time 400 msec, 2x2 binning) with a Hamamatsu Orca ER 12 bit digital camera mounted on a spinning disk confocal microscope (Zeiss Axioplan using a 63x 1.4 NA PlanApochromat objective and Yokogawa disk head). Illumination was via a 488nm Argon ion laser (Melles Griot). Movies acquired for Figure 2 were done on a wide-field microscope (Zeiss Axioplan II using a 63x 1.4 NA PlanApochromat objective equipped with a Hamamatsu Orca ER 12 bit digital camera). Image processing was done with MetaView Software (Universal Imaging Corporation).

Immunofluorescence

Immunolocalization was performed using a modified method from (Gonczy et al., 1999). Briefly, 10-20 adult hermaphrodites were placed in a drop of water on polylysine-coated glass slides (Sigma). The embryos were dissected from the animal gonad with a needle. A coverslip was gently placed on top of the dissected worms, and the slides were placed in liquid nitrogen for 10 min. After the coverslips were snapped off with a scalpel, the slides were immediately placed in -20 °C Methanol for 12 min. The embryos were rehydrated in 2xPBS for 10 min and then incubated with primary antibodies with 5% donkey serum for 1-2 hours at room temperature. Before incubation with secondary antibodies, the slides were washed in 1xPBST (0.05% Tween 20) for 10 min. After the secondary antibody incubation for 1 hour at room temperature in the dark, the slides were washed 10 min in 1xPBST and 10 min in 1xPBS. The coverslips were mounted with 5 µl mounting media (0.5% p-phenylenediamine, 20 mM Tris-Cl, pH 8.8, 90% glycerol) that had been premixed with 1 µg/ml 4',6-diamidino-2-phenylindole (DAPI). The slides were left at 4 °C over night before sealing with nail polish.

For the PAR-2 immunostaining the GFP::PAR-2 strain (JH1380) was used. A sheep polyclonal antibody to GFP (1:1000; a gift from Francis Barr, Max-Planck-Institute of Biochemistry, Martinsried, Germany) was used to visualize PAR-2. DM1α (1:300, Sigma) and SPD-2 (1:5000; (Pelletier et al., 2004)) was used to detect microtubules and centrosomes. Actin was stained with a mouse monoclonal anti-actin antibody (1:50; clone C4; Chemicon International). The anti-K09H11.3 antibody was used at 1:500 (a gift from Karen Oegema, University of California, San Diego, Ludwig Institute for Cancer Research, La Jolla, USA). The antibodies were visualized with FITC-, TR-,

Cy5-conjugated antibodies (Jackson Immunochemicals) and with a donkey anti-sheep antibody coupled to Alexa 488 (Molecular Probes). For some multicolor immunolocalization studies, directly labeled antibodies were used. Direct labeling of antibodies was performed as described (Francis-Lang et al. 1999). SPD-5 was stained with an anti-SPD-5 antibody (Pelletier et al., 2004) directly labeled with CY3 (1: 500), AIR-1 was visualized with an anti-AIR-1 antibody (Hannak et al., 2001) directly labeled with CY3 (1:250), the anti-K09H11.3 antibody directly labeled with CY5 was used at 1:200 and Dm1α directly labeled with FITC was used at 1:300. Imaging was performed on a DeltaVision microscope and stacks were deconvolved (Applied Precision) as described (Oegema et al., 2001).

Antibody production

To make a GST fusion protein to generate an antibody to a C-terminal fragment of K09H11.3, the following primers were used to amplify from cDNA: CGCGCGGGATCCACTTTCTCGCCGAAACTGC, CGCGCGCTCGAGTTAGAAATATTGC-CCAGCATCA. The antibody was raised and purified as described (Oegema et al., 2001).

Contractility tracking

The ruffle kymographs were performed as described (Cowan et al. 2004). Briefly, the ruffles were tracked starting around the time of beginning of pronuclear appearance for an interval of 1000 seconds. The position of cortical ruffles was manually tracked and projected onto a calculated ellipse. One half of the ellipse was straightened to generate the x-axis, the anterior-posterior axis. This procedure was done for each time point and laid down sequentially along the y-axis (time). Lines connect ruffles within nearest neighbor groups. The embryo length along the anterior (ANT) -posterior (POST) axis was standardized to 1.

Tracking of PAR-2 and PAR-6 domain extent

The extent of the GFP::PAR-2 domain was manually tracked after the domain reached its maximal size. The extent of the GFP::PAR-6 domain was tracked after pseudocleavage regression. The domain size was calculated as a fraction of the respective embryo circumference. Manual tracking was performed using a custom-written macro (Stephan Grill) for NIH-Image (NIH). Further analysis was done with Mathematica 4.1 (Wolfram Research).

Tracking of NMY-2::GFP foci

GFP::NMY-2 foci were manually tracked with Metamorph Software (Universal Imaging Corporation).

Kymograph analysis

Kymographs were done with Metamorph Software (Universal Imaging Corporation) from time-lapse DIC and GFP recordings (12-15 min total). Kymographs were made from a curved line along the embryo cortex, centered on the location of initial PAR-2::GFP appearance. The red star marks the left side of the kymographs. For the overlay of the borders of both GFP::PAR-2 domains from kymographs (Figure 10A and B), left side of both borders was aligned (Figure 10D).

Calculation of pseudocleavage furrow position

Position of pseudocleavage furrow was measured as a distance along the long axis of the embryo. The distance was standardized to the total length of the embryo and was expressed as percentage of embryo length. 0% indicates posterior pole.

Kymograph analysis of Par-2 domain extent and position of pseudocleavage furrow

The ruffle kymographs were performed as described (Cowan et al. 2004). Briefly, the tracking starts around the time of beginning of pronuclear appearance for an interval of 800-1000 seconds. The position of the GFP::PAR-2 domain boundary, of the pseudocleavage furrow and of the pronuclei was tracked manually. The embryo length along the anterior (ANT) – posterior (POST) axis was standardized to 1. The positions of PAR-2 boundaries (solid green line), pseudocleavage furrow (red dots) and of pronuclei (blue dots) were projected onto the anterior (ANT) – posterior (POST) axis, displayed as the x-axis of the graphs. The positions were plotted for each time point, represented along the y-axis.

5. APPENDIX

Supplemental movies.

QuickTime movies are on the enclosed CD. Embryo posterior is to the right.

Movie S1.   Cortical NMY-2::GFP dynamics of a wild-type embryo.

Movie S2.   Cortical NMY-2::GFP dynamics in a *cdc-42(RNAi)* embryo.

Movie S3.   GFP::PAR-2 dynamics of a wild-type embryo.

Movie S4.   GFP::PAR-2 dynamics in a *cdc-42(RNAi)* embryo.

Movie S5.   GFP::PAR-6 dynamics of a wild-type embryo

Movie S6.   GFP::PAR-6 dynamics in a *cdc-42(RNAi)* embryo.

Movie S7.   YFP::CDC-42 dynamics of a wild-type embryo (center).

Movie S8.   Cortical YFP::CDC-42 dynamics of a wild-type embryo.

Movie S9.   Cortical YFP::CDC-42 dynamics in a *par-3(RNAi)* embryo.

Movie S10.   Cortical YFP::CDC-42 dynamics in a *par-6(RNAi)* embryo.

Movie S11.   GFP::PAR-6 dynamics in a *rho-1(RNAi)* embryo.

Movie S12.   GFP::PAR-2 dynamics in a *rho-1(RNAi)* embryo.

Movie S13.   GFP::PAR-2 dynamics in an *ect-2(RNAi)* embryo.

Movie S14.   GFP::PAR-2 dynamics in an *ect-2(RNAi)* embryo.
(no GFP::PAR-2 localization at the cortex)

Movie S15.   GFP::PAR-6 dynamics in an *ect-2(RNAi)* embryo.

Movie S16.   Cortical NMY-2::GFP dynamics in an *ect-2(RNAi)* embryo.

Movie S17.   Cortical NMY-2::GFP;GFP::PAR-2 dynamics of a wild-type embryo.

Movie S18.   Cortical NMY-2::GFP;GFP::PAR-2 dynamics in an *ect-2(RNAi)* embryo.

Movie S19.   Cortical YFP::CDC-42 dynamics in a *ect-2(RNAi)* embryo.

Movie S20.   GFP::PAR-2 dynamics in a *cdc-42(RNAi);rho-1(RNAi)* embryo.

Movie S21.   GFP::PAR-6 dynamics in a *cdc-42(RNAi);rho-1(RNAi)* embryo.

Movie S22.   NMY-2::GFP dynamics in an *K09H11.3(RNAi)* embryo.

Movie S23.   GFP::PAR-2 dynamics in a *K09H11.3(RNAi)* embryo.

Movie S24.   GFP::PAR-6 dynamics in a *K09H11.3(RNAi)* embryo.

Movie S25.   GFP::PAR-2 dynamics in a *K09H11.3(RNAi);rho-1(RNAi)* embryo.

Movie S26.   GFP::PAR-6 dynamics in a *K09H11.3(RNAi);rho-1(RNAi)* embryo.

Movie S27.   GFP::PAR-2 dynamics in a *K09H11.3(RNAi);cdc-42(RNAi)* embryo.

Movie S28.   GFP::PAR-6 dynamics in a *K09H11.3(RNAi);cdc-42(RNAi)* embryo.

6. ABBREVIATIONS

A/P	Anterior-posterior
DIC	Differential interference contrast
DsRNA	Double-stranded RNA
GAP	GTPase Activating Protein
GEF	Guanine nucleotide Exchange Factor
GFP	Green Fluorescent Protein
MT	Microtubule
NEBD	Nuclear Envelop Breakdown
NMY-2	non-muscle myosin II
MLC-4	Myosin light regulatory chain 4
PAR	Partitioning-defective
PBS	Phosphate buffered saline
PCM	Pericentriolar Material
PSCF	Pseudocleavage furrow
RNAi	RNA-mediated interference
YFP	Yellow Fluorescent Protein

7. ACKNOWLEDMENTS

8. REFERENCES

Adams, A. E., Johnson, D. I., Longnecker, R. M., Sloat, B. F., and Pringle, J. R. (1990). CDC42 and CDC43, two additional genes involved in budding and the establishment of cell polarity in the yeast Saccharomyces cerevisiae. J Cell Biol *111*, 131-142.

Ahmed, S., Lee, J., Kozma, R., Best, A., Monfries, C., and Lim, L. (1993). A novel functional target for tumor-promoting phorbol esters and lysophosphatidic acid. The p21rac-GTPase activating protein n-chimaerin. J Biol Chem *268*, 10709-10712.

Aktories, K., and Hall, A. (1989). Botulinum ADP-ribosyltransferase C3: a new tool to study low molecular weight GTP-binding proteins. Trends Pharmacol Sci *10*, 415-418.

Aspenstrom, P., Fransson, A., and Saras, J. (2004). Rho GTPases have diverse effects on the organization of the actin filament system. Biochem J *377*, 327-337.

Bernards, A. (2003). GAPs galore! A survey of putative Ras superfamily GTPase activating proteins in man and Drosophila. Biochim Biophys Acta *1603*, 47-82.

Billuart, P., Winter, C. G., Maresh, A., Zhao, X., and Luo, L. (2001). Regulating axon branch stability: the role of p190 RhoGAP in repressing a retraction signaling pathway. Cell *107*, 195-207.

Bowerman, B. (2000). Embryonic polarity: protein stability in asymmetric cell division. Curr Biol *10*, R637-641.

Boyd, L., Guo, S., Levitan, D., Stinchcomb, D. T., and Kemphues, K. J. (1996). PAR-2 is asymmetrically distributed and promotes association of P granules and PAR-1 with the cortex in C. elegans embryos. Development *122*, 3075-3084.

Brenner, S. (1974). The genetics of Caenorhabditis elegans. Genetics *77*, 71-94.

Bretscher, A. (1991). Microfilament structure and function in the cortical cytoskeleton. Annu Rev Cell Biol *7*, 337-374.

Bretscher, A. (2003). Polarized growth and organelle segregation in yeast: the tracks, motors, and receptors. J Cell Biol *160*, 811-816.

Bryan, B. A., Li, D., Wu, X., and Liu, M. (2005). The Rho family of small GTPases: crucial regulators of skeletal myogenesis. Cell Mol Life Sci *62*, 1547-1555.

Caruso, M. E., Jenna, S., Beaulne, S., Lee, E. H., Bergeron, A., Chauve, C., Roby, P., Rual, J. F., Hill, D. E., Vidal, M.*, et al.* (2005). Biochemical Clustering of Monomeric GTPases of the Ras Superfamily. Mol Cell Proteomics *4*, 936-944.

Chang, F., Drubin, D., and Nurse, P. (1997). cdc12p, a protein required for cytokinesis in fission yeast, is a component of the cell division ring and interacts with profilin. J Cell Biol *137*, 169-182.

Cheeks, R. J., Canman, J. C., Gabriel, W. N., Meyer, N., Strome, S., and Goldstein, B. (2004). C. elegans PAR proteins function by mobilizing and stabilizing asymmetrically localized protein complexes. Curr Biol *14*, 851-862.

Chen, W., and Lim, L. (1994). The Caenorhabditis elegans small GTP-binding protein RhoA is enriched in the nerve ring and sensory neurons during larval development. J Biol Chem *269*, 32394-32404.

Cheng, N. N., Kirby, C. M., and Kemphues, K. J. (1995). Control of cleavage spindle orientation in Caenorhabditis elegans: the role of the genes par-2 and par-3. Genetics *139*, 549-559.

Cowan, C. R., and Hyman, A. A. (2004a). Asymmetric cell division in C. elegans: cortical polarity and spindle positioning. Annu Rev Cell Dev Biol *20*, 427-453.

Cowan, C. R., and Hyman, A. A. (2004b). Centrosomes direct cell polarity independently of microtubule assembly in C. elegans embryos. Nature *431*, 92-96.

Cuenca, A. A., Schetter, A., Aceto, D., Kemphues, K., and Seydoux, G. (2003). Polarization of the C. elegans zygote proceeds via distinct establishment and maintenance phases. Development *130*, 1255-1265.

Dong, Y., Pruyne, D., and Bretscher, A. (2003). Formin-dependent actin assembly is regulated by distinct modes of Rho signaling in yeast. J Cell Biol *161*, 1081-1092.

Drechsel, D. N., Hyman, A. A., Hall, A., and Glotzer, M. (1997). A requirement for Rho and Cdc42 during cytokinesis in Xenopus embryos. Curr Biol *7*, 12-23.

Drubin, D. G., and Nelson, W. J. (1996). Origins of cell polarity. Cell *84*, 335-344.

Etemad-Moghadam, B., Guo, S., and Kemphues, K. J. (1995). Asymmetrically distributed PAR-3 protein contributes to cell polarity and spindle alignment in early C. elegans embryos. Cell *83*, 743-752.

Etienne-Manneville, S. (2004). Cdc42--the centre of polarity. J Cell Sci *117*, 1291-1300.

Etienne-Manneville, S., and Hall, A. (2001). Integrin-mediated activation of Cdc42 controls cell polarity in migrating astrocytes through PKCzeta. Cell *106*, 489-498.

Etienne-Manneville, S., and Hall, A. (2002). Rho GTPases in cell biology. Nature *420*, 629-635.

Etienne-Manneville, S., and Hall, A. (2003a). Cdc42 regulates GSK-3beta and adenomatous polyposis coli to control cell polarity. Nature *421*, 753-756.

Etienne-Manneville, S., and Hall, A. (2003b). Cell polarity: Par6, aPKC and cytoskeletal crosstalk. Curr Opin Cell Biol *15*, 67-72.

Fire, A., Xu, S., Montgomery, M. K., Kostas, S. A., Driver, S. E., and Mello, C. C. (1998). Potent and specific genetic interference by double-stranded RNA in Caenorhabditis elegans. Nature *391*, 806-811.

Fraser, A. G., Kamath, R. S., Zipperlen, P., Martinez-Campos, M., Sohrmann, M., and Ahringer, J. (2000). Functional genomic analysis of C. elegans chromosome I by systematic RNA interference. Nature *408*, 325-330.

Fukata, M., Nakagawa, M., and Kaibuchi, K. (2003). Roles of Rho-family GTPases in cell polarisation and directional migration. Curr Opin Cell Biol *15*, 590-597.

Garrard, S. M., Capaldo, C. T., Gao, L., Rosen, M. K., Macara, I. G., and Tomchick, D. R. (2003). Structure of Cdc42 in a complex with the GTPase-binding domain of the cell polarity protein, Par6. Embo J *22*, 1125-1133.

Giansanti, M. G., Bonaccorsi, S., Williams, B., Williams, E. V., Santolamazza, C., Goldberg, M. L., and Gatti, M. (1998). Cooperative interactions between the central spindle and the contractile ring during Drosophila cytokinesis. Genes Dev *12*, 396-410.

Glotzer, M. (2005). The molecular requirements for cytokinesis. Science *307*, 1735-1739.

Golden, A. (2000). Cytoplasmic flow and the establishment of polarity in C. elegans 1-cell embryos. Curr Opin Genet Dev *10*, 414-420.

Goldstein, B., and Hird, S. N. (1996). Specification of the anteroposterior axis in Caenorhabditis elegans. Development *122*, 1467-1474.

Gonczy, P., Echeverri, C., Oegema, K., Coulson, A., Jones, S. J., Copley, R. R., Duperon, J., Oegema, J., Brehm, M., Cassin, E.*, et al.* (2000). Functional genomic analysis of cell division in C. elegans using RNAi of genes on chromosome III. Nature *408*, 331-336.

Gonczy, P., Schnabel, H., Kaletta, T., Amores, A. D., Hyman, T., and Schnabel, R. (1999). Dissection of cell division processes in the one cell stage Caenorhabditis elegans embryo by mutational analysis. J Cell Biol *144*, 927-946.

Gotta, M., Abraham, M. C., and Ahringer, J. (2001). CDC-42 controls early cell polarity and spindle orientation in C. elegans. Curr Biol *11*, 482-488.

Gotta, M., and Ahringer, J. (2001). Axis determination in C. elegans: initiating and transducing polarity. Curr Opin Genet Dev *11*, 367-373.

Guo, S., and Kemphues, K. J. (1995). par-1, a gene required for establishing polarity in C. elegans embryos, encodes a putative Ser/Thr kinase that is asymmetrically distributed. Cell *81*, 611-620. Guo, S., and Kemphues, K. J. (1996a). Molecular genetics of asymmetric cleavage in the early Caenorhabditis elegans embryo. Curr Opin Genet Dev *6*, 408-415.

Guo, S., and Kemphues, K. J. (1996b). A non-muscle myosin required for embryonic polarity in Caenorhabditis elegans. Nature *382*, 455-458.

Haarer, B. K., Lillie, S. H., Adams, A. E., Magdolen, V., Bandlow, W., and Brown, S. S. (1990). Purification of profilin from Saccharomyces cerevisiae and analysis of profilin-deficient cells. J Cell Biol *110*, 105-114.

Hamill, D. R., Severson, A. F., Carter, J. C., and Bowerman, B. (2002). Centrosome maturation and mitotic spindle assembly in C. elegans require SPD-5, a protein with multiple coiled-coil domains. Dev Cell *3*, 673-684.

Hannak, E., Kirkham, M., Hyman, A. A., and Oegema, K. (2001). Aurora-A kinase is required for centrosome maturation in Caenorhabditis elegans. J Cell Biol *155*, 1109-1116.

Henrique, D., and Schweisguth, F. (2003). Cell polarity: the ups and downs of the Par6/aPKC complex. Curr Opin Genet Dev *13*, 341-350.

Hill, D. P., and Strome, S. (1988). An analysis of the role of microfilaments in the establishment and maintenance of asymmetry in Caenorhabditis elegans zygotes. Dev Biol *125*, 75-84.

Hill, D. P., and Strome, S. (1990). Brief cytochalasin-induced disruption of microfilaments during a critical interval in 1-cell C. elegans embryos alters the partitioning of developmental instructions to the 2-cell embryo. Development *108*, 159-172.

Hird, S. N., and White, J. G. (1993). Cortical and cytoplasmic flow polarity in early embryonic cells of Caenorhabditis elegans. J Cell Biol *121*, 1343-1355.

Hirsh, D., Oppenheim, D., and Klass, M. (1976). Development of the reproductive system of Caenorhabditis elegans. Dev Biol *49*, 200-219.

Hung, T. J., and Kemphues, K. J. (1999). PAR-6 is a conserved PDZ domain-containing protein that colocalizes with PAR-3 in Caenorhabditis elegans embryos. Development *126*, 127-135.

Hutterer, A., Betschinger, J., Petronczki, M., and Knoblich, J. A. (2004). Sequential roles of Cdc42, Par-6, aPKC, and Lgl in the establishment of epithelial polarity during Drosophila embryogenesis. Dev Cell *6*, 845-854.

Imamura, H., Tanaka, K., Hihara, T., Umikawa, M., Kamei, T., Takahashi, K., Sasaki, T., and Takai, Y. (1997). Bni1p and Bnr1p: downstream targets of the Rho family small G-proteins which interact with profilin and regulate actin cytoskeleton in Saccharomyces cerevisiae. Embo J *16*, 2745-2755.

Izumi, Y., Hirose, T., Tamai, Y., Hirai, S., Nagashima, Y., Fujimoto, T., Tabuse, Y., Kemphues, K. J., and Ohno, S. (1998). An atypical PKC directly associates and colocalizes at the epithelial tight junction with ASIP, a mammalian homologue of Caenorhabditis elegans polarity protein PAR-3. J Cell Biol *143*, 95-106.

Jaffe, A. B., and Hall, A. (2005). Rho GTPases: Biochemestry and Biology. Annu Rev Cell Dev Biol *21*, 247-269.

Jantsch-Plunger, V., Gonczy, P., Romano, A., Schnabel, H., Hamill, D., Schnabel, R., Hyman, A. A., and Glotzer, M. (2000). CYK-4: A Rho family gtpase activating protein (GAP) required for central spindle formation and cytokinesis. J Cell Biol *149*, 1391-1404.

Jenna, S., Caruso, M. E., Emadali, A., Nguyen, D. T., Dominguez, M., Li, S., Roy, R., Reboul, J., Vidal, M., Tzimas, G. N.*, et al.* (2005). Regulation of membrane trafficking by a novel Cdc42-related protein in Caenorhabditis elegans epithelial cells. Mol Biol Cell *16*, 1629-1639.

Jenna, S., Hussain, N. K., Danek, E. I., Triki, I., Wasiak, S., McPherson, P. S., and Lamarche-Vane, N. (2002). The activity of the GTPase-activating protein CdGAP is regulated by the endocytic protein intersectin. J Biol Chem *277*, 6366-6373.

Joberty, G., Petersen, C., Gao, L., and Macara, I. G. (2000). The cell-polarity protein Par6 links Par3 and atypical protein kinase C to Cdc42. Nat Cell Biol *2*, 531-539.

Johansson, A., Driessens, M., and Aspenstrom, P. (2000). The mammalian homologue of the Caenorhabditis elegans polarity protein PAR-6 is a binding partner for the Rho GTPases Cdc42 and Rac1. J Cell Sci *113 (Pt 18)*, 3267-3275.

Johnson, D. I. (1999). Cdc42: An essential Rho-type GTPase controlling eukaryotic cell polarity. Microbiol Mol Biol Rev *63*, 54-105.

Johnson, D. I., and Pringle, J. R. (1990). Molecular characterization of CDC42, a Saccharomyces cerevisiae gene involved in the development of cell polarity. J Cell Biol *111*, 143-152.

Kay, A. J., and Hunter, C. P. (2001). CDC-42 regulates PAR protein localization and function to control cellular and embryonic polarity in C. elegans. Curr Biol *11*, 474-481.

Kemphues, K. J., Priess, J. R., Morton, D. G., and Cheng, N. S. (1988). Identification of genes required for cytoplasmic localization in early C. elegans embryos. Cell *52*, 311-320.

Kirby, C., Kusch, M., and Kemphues, K. (1990). Mutations in the par genes of Caenorhabditis elegans affect cytoplasmic reorganization during the first cell cycle. Dev Biol *142*, 203-215.

Kishi, K., Sasaki, T., Kuroda, S., Itoh, T., and Takai, Y. (1993). Regulation of cytoplasmic division of Xenopus embryo by rho p21 and its inhibitory GDP/GTP exchange protein (rho GDI). J Cell Biol *120*, 1187-1195.

Knoblich, J. A. (2001). Asymmetric cell division during animal development. Nat Rev Mol Cell Biol *2*, 11-20.

Kozma, R., Ahmed, S., Best, A., and Lim, L. (1995). The Ras-related protein Cdc42Hs and bradykinin promote formation of peripheral actin microspikes and filopodia in Swiss 3T3 fibroblasts. Mol Cell Biol *15*, 1942-1952.

Kozma, R., Ahmed, S., Best, A., and Lim, L. (1996). The GTPase-activating protein n-chimaerin cooperates with Rac1 and Cdc42Hs to induce the formation of lamellipodia and filopodia. Mol Cell Biol *16*, 5069-5080.

Lang, P., Gesbert, F., Delespine-Carmagnat, M., Stancou, R., Pouchelet, M., and Bertoglio, J. (1996). Protein kinase A phosphorylation of RhoA mediates the morphological and functional effects of cyclic AMP in cytotoxic lymphocytes. Embo J *15*, 510-519.
Lehner, C. F. (1992). The pebble gene is required for cytokinesis in Drosophila. J Cell Sci *103 (Pt 4)*, 1021-1030.

Levitan, D. J., Boyd, L., Mello, C. C., Kemphues, K. J., and Stinchcomb, D. T. (1994). par-2, a gene required for blastomere asymmetry in Caenorhabditis elegans, encodes zinc-finger and ATP-binding motifs. Proc Natl Acad Sci U S A *91*, 6108-6112.

Lin, D., Edwards, A. S., Fawcett, J. P., Mbamalu, G., Scott, J. D., and Pawson, T. (2000). A mammalian PAR-3-PAR-6 complex implicated in Cdc42/Rac1 and aPKC signalling and cell polarity. Nat Cell Biol *2*, 540-547.

Liu, X. F., Ishida, H., Raziuddin, R., and Miki, T. (2004). Nucleotide exchange factor ECT2 interacts with the polarity protein complex Par6/Par3/protein kinase Czeta (PKCzeta) and regulates PKCzeta activity. Mol Cell Biol *24*, 6665-6675.

Lundquist, E. A., Reddien, P. W., Hartwieg, E., Horvitz, H. R., and Bargmann, C. I. (2001). Three C. elegans Rac proteins and several alternative Rac regulators control axon guidance, cell migration and apoptotic cell phagocytosis. Development *128*, 4475-4488.

Mabuchi, I., Hamaguchi, Y., Fujimoto, H., Morii, N., Mishima, M., and Narumiya, S. (1993). A rho-like protein is involved in the organisation of the contractile ring in dividing sand dollar eggs. Zygote *1*, 325-331.

Macara, I. G. (2004). Parsing the polarity code. Nat Rev Mol Cell Biol *5*, 220-231.

Machesky, L. M., and Gould, K. L. (1999). The Arp2/3 complex: a multifunctional actin organizer. Curr Opin Cell Biol *11*, 117-121.

May, R. C. (2001). The Arp2/3 complex: a central regulator of the actin cytoskeleton. Cell Mol Life Sci *58*, 1607-1626.

Minoshima, Y., Kawashima, T., Hirose, K., Tonozuka, Y., Kawajiri, A., Bao, Y. C., Deng, X., Tatsuka, M., Narumiya, S., May, W. S., Jr.*, et al.* (2003). Phosphorylation by aurora B converts MgcRacGAP to a RhoGAP during cytokinesis. Dev Cell *4*, 549-560.

Moorman, J. P., Bobak, D. A., and Hahn, C. S. (1996). Inactivation of the small GTP binding protein Rho induces multinucleate cell formation and apoptosis in murine T lymphoma EL4. J Immunol *156*, 4146-4153.

Morton, D. G., Shakes, D. C., Nugent, S., Dichoso, D., Wang, W., Golden, A., and Kemphues, K. J. (2002). The Caenorhabditis elegans par-5 gene encodes a 14-3-3 protein required for cellular asymmetry in the early embryo. Dev Biol *241*, 47-58.

Munro, E., Nance, J., and Priess, J. R. (2004). Cortical flows powered by asymmetrical contraction transport PAR proteins to establish and maintain anterior-posterior polarity in the early C. elegans embryo. Dev Cell *7*, 413-424.

O'Connell, K. F., Maxwell, K. N., and White, J. G. (2000). The spd-2 gene is required for polarization of the anteroposterior axis and formation of the sperm asters in the Caenorhabditis elegans zygote. Dev Biol *222*, 55-70.

Oegema, K., Desai, A., Rybina, S., Kirkham, M., and Hyman, A. A. (2001). Functional analysis of kinetochore assembly in Caenorhabditis elegans. J Cell Biol *153*, 1209-1226.

Ohno, S. (2001). Intercellular junctions and cellular polarity: the PAR-aPKC complex, a conserved core cassette playing fundamental roles in cell polarity. Curr Opin Cell Biol *13*, 641-648.

Olofsson, B. (1999). Rho guanine dissociation inhibitors: pivotal molecules in cellular signalling. Cell Signal *11*, 545-554.

Pelletier, L., Ozlu, N., Hannak, E., Cowan, C., Habermann, B., Ruer, M., Muller-Reichert, T., and Hyman, A. A. (2004). The Caenorhabditis elegans centrosomal protein SPD-2 is required for both pericentriolar material recruitment and centriole duplication. Curr Biol *14*, 863-873.

Petronczki, M., and Knoblich, J. A. (2001). DmPAR-6 directs epithelial polarity and asymmetric cell division of neuroblasts in Drosophila. Nat Cell Biol *3*, 43-49.

Piekny, A. J., and Mains, P. E. (2002). Rho-binding kinase (LET-502) and myosin phosphatase (MEL-11) regulate cytokinesis in the early Caenorhabditis elegans embryo. J Cell Sci *115*, 2271-2282.

Pollard, T. D. (1986). Assembly and dynamics of the actin filament system in nonmuscle cells. J Cell Biochem *31*, 87-95.

Pollard, T. D., Blanchoin, L., and Mullins, R. D. (2000). Molecular mechanisms controlling actin filament dynamics in nonmuscle cells. Annu Rev Biophys Biomol Struct *29*, 545-576.

Pollard, T. D., and Borisy, G. G. (2003). Cellular motility driven by assembly and disassembly of actin filaments. Cell *112*, 453-465.

Praitis, V., Casey, E., Collar, D., and Austin, J. (2001). Creation of low-copy integrated transgenic lines in Caenorhabditis elegans. Genetics *157*, 1217-1226.

Prokopenko, S. N., Brumby, A., O'Keefe, L., Prior, L., He, Y., Saint, R., and Bellen, H. J. (1999). A putative exchange factor for Rho1 GTPase is required for initiation of cytokinesis in Drosophila. Genes Dev *13*, 2301-2314.

Pruyne, D., and Bretscher, A. (2000). Polarization of cell growth in yeast. I. Establishment and maintenance of polarity states. J Cell Sci *113 (Pt 3)*, 365-375.

Qiu, R. G., Abo, A., and Steven Martin, G. (2000). A human homolog of the C. elegans polarity determinant Par-6 links Rac and Cdc42 to PKCzeta signaling and cell transformation. Curr Biol *10*, 697-707.

Rappleye, C. A., Paredez, A. R., Smith, C. W., McDonald, K. L., and Aroian, R. V. (1999). The coronin-like protein POD-1 is required for anterior-posterior axis formation and cellular architecture in the nematode caenorhabditis elegans. Genes Dev *13*, 2838-2851.

Reddien, P. W., and Horvitz, H. R. (2000). CED-2/CrkII and CED-10/Rac control phagocytosis and cell migration in Caenorhabditis elegans. Nat Cell Biol *2*, 131-136.

Revenu, C., Athman, R., Robine, S., and Louvard, D. (2004). The co-workers of actin filaments: from cell structures to signals. Nat Rev Mol Cell Biol *5*, 635-646.

Ridley, A. J., and Hall, A. (1992). The small GTP-binding protein rho regulates the assembly of focal adhesions and actin stress fibers in response to growth factors. Cell *70*, 389-399.

Ridley, A. J., Paterson, H. F., Johnston, C. L., Diekmann, D., and Hall, A. (1992). The small GTP-binding protein rac regulates growth factor-induced membrane ruffling. Cell *70*, 401-410.

Rohatgi, R., Ma, L., Miki, H., Lopez, M., Kirchhausen, T., Takenawa, T., and Kirschner, M. W. (1999). The interaction between N-WASP and the Arp2/3 complex links Cdc42-dependent signals to actin assembly. Cell *97*, 221-231.

Roof, R. W., Haskell, M. D., Dukes, B. D., Sherman, N., Kinter, M., and Parsons, S. J. (1998). Phosphotyrosine (p-Tyr)-dependent and -independent mechanisms of p190 RhoGAP-p120 RasGAP interaction: Tyr 1105 of p190, a substrate for c-Src, is the sole p-Tyr mediator of complex formation. Mol Cell Biol *18*, 7052-7063.

Rose, L. S., and Kemphues, K. J. (1998). Early patterning of the C. elegans embryo. Annu Rev Genet *32*, 521-545.

Sadler, P. L., and Shakes, D. C. (2000). Anucleate Caenorhabditis elegans sperm can crawl, fertilize oocytes and direct anterior-posterior polarization of the 1-cell embryo. Development *127*, 355-366.

Sawa, M., Suetsugu, S., Sugimoto, A., Miki, H., Yamamoto, M., and Takenawa, T. (2003). Essential role of the C. elegans Arp2/3 complex in cell migration during ventral enclosure. J Cell Sci *116*, 1505-1518.

Schmidt, A., and Hall, A. (2002). Guanine nucleotide exchange factors for Rho GTPases: turning on the switch. Genes Dev *16*, 1587-1609.

Schneider, S. Q., and Bowerman, B. (2003). Cell polarity and the cytoskeleton in the Caenorhabditis elegans zygote. Annu Rev Genet *37*, 221-249.

Schober, M., Schaefer, M., and Knoblich, J. A. (1999). Bazooka recruits Inscuteable to orient asymmetric cell divisions in Drosophila neuroblasts. Nature *402*, 548-551.

Severson, A. F., Baillie, D. L., and Bowerman, B. (2002). A Formin Homology protein and a profilin are required for cytokinesis and Arp2/3-independent assembly of cortical microfilaments in C. elegans. Curr Biol *12*, 2066-2075.

Severson, A. F., and Bowerman, B. (2003). Myosin and the PAR proteins polarize microfilament-dependent forces that shape and position mitotic spindles in Caenorhabditis elegans. J Cell Biol *161*, 21-26.

Shelton, C. A., Carter, J. C., Ellis, G. C., and Bowerman, B. (1999). The nonmuscle myosin regulatory light chain gene mlc-4 is required for cytokinesis, anterior-posterior polarity, and body morphology during Caenorhabditis elegans embryogenesis. J Cell Biol *146*, 439-451.

Sonnichsen, B., Koski, L. B., Walsh, A., Marschall, P., Neumann, B., Brehm, M., Alleaume, A. M., Artelt, J., Bettencourt, P., Cassin, E.*, et al.* (2005). Full-genome RNAi profiling of early embryogenesis in Caenorhabditis elegans. Nature *434*, 462-469.

Spencer, A. G., Orita, S., Malone, C. J., and Han, M. (2001). A RHO GTPase-mediated pathway is required during P cell migration in Caenorhabditis elegans. Proc Natl Acad Sci U S A *98*, 13132-13137.

Stowers, L., Yelon, D., Berg, L. J., and Chant, J. (1995). Regulation of the polarization of T cells toward antigen-presenting cells by Ras-related GTPase CDC42. Proc Natl Acad Sci U S A *92*, 5027-5031.

Strome, S. (1986). Fluorescence visualization of the distribution of microfilaments in gonads and early embryos of the nematode Caenorhabditis elegans. J Cell Biol *103*, 2241-2252.

Strome, S., and Hill, D. P. (1988). Early embryogenesis in Caenorhabditis elegans: the cytoskeleton and spatial organization of the zygote. Bioessays *8*, 145-149.

Swan, K. A., Severson, A. F., Carter, J. C., Martin, P. R., Schnabel, H., Schnabel, R., and Bowerman, B. (1998). cyk-1: a C. elegans FH gene required for a late step in embryonic cytokinesis. J Cell Sci *111 (Pt 14)*, 2017-2027.

Tabuse, Y., Izumi, Y., Piano, F., Kemphues, K. J., Miwa, J., and Ohno, S. (1998). Atypical protein kinase C cooperates with PAR-3 to establish embryonic polarity in Caenorhabditis elegans. Development *125*, 3607-3614.

Takenawa, T., and Miki, H. (2001). WASP and WAVE family proteins: key molecules for rapid rearrangement of cortical actin filaments and cell movement. J Cell Sci *114*, 1801-1809.

Tatsumoto, T., Xie, X., Blumenthal, R., Okamoto, I., and Miki, T. (1999). Human ECT2 is an exchange factor for Rho GTPases, phosphorylated in G2/M phases, and involved in cytokinesis. J Cell Biol *147*, 921-928.

Timmons, L., and Fire, A. (1998). Specific interference by ingested dsRNA. Nature *395*, 854.

Tzima, E., Kiosses, W. B., del Pozo, M. A., and Schwartz, M. A. (2003). Localized cdc42 activation, detected using a novel assay, mediates microtubule organizing center positioning in endothelial cells in response to fluid shear stress. J Biol Chem *278*, 31020-31023.

Wallar, B. J., and Alberts, A. S. (2003). The formins: active scaffolds that remodel the cytoskeleton. Trends Cell Biol *13*, 435-446.

Wang, H., and Chia, W. (2005). Drosophila neural progenitor polarity and asymmetric division. Biol Cell *97*, 63-74.

Wang, H. R., Zhang, Y., Ozdamar, B., Ogunjimi, A. A., Alexandrova, E., Thomsen, G. H., and Wrana, J. L. (2003). Regulation of cell polarity and protrusion formation by targeting RhoA for degradation. Science *302*, 1775-1779.

Watts, J. L., Etemad-Moghadam, B., Guo, S., Boyd, L., Draper, B. W., Mello, C. C., Priess, J. R., and Kemphues, K. J. (1996). par-6, a gene involved in the establishment of asymmetry in early C. elegans embryos, mediates the asymmetric localization of PAR-3. Development *122*, 3133-3140.

Watts, J. L., Morton, D. G., Bestman, J., and Kemphues, K. J. (2000). The C. elegans par-4 gene encodes a putative serine-threonine kinase required for establishing embryonic asymmetry. Development *127*, 1467-1475.

Welch, M. D., Iwamatsu, A., and Mitchison, T. J. (1997). Actin polymerization is induced by Arp2/3 protein complex at the surface of Listeria monocytogenes. Nature *385*, 265-269.

Wherlock, M., and Mellor, H. (2002). The Rho GTPase family: a Racs to Wrchs story. J Cell Sci *115*, 239-240.

Witke, W. (2004). The role of profilin complexes in cell motility and other cellular processes. Trends Cell Biol *14*, 461-469.

Wodarz, A., Ramrath, A., Kuchinke, U., and Knust, E. (1999). Bazooka provides an apical cue for Inscuteable localization in Drosophila neuroblasts. Nature *402*, 544-547.

Wood, W. B. (1988). The Nematode Caenorhabditis elegans: Cold Spring Harbor Laboratory Press, New York. 1-16).

Wu, Y. C., Cheng, T. W., Lee, M. C., and Weng, N. Y. (2002). Distinct rac activation pathways control Caenorhabditis elegans cell migration and axon outgrowth. Dev Biol *250*, 145-155.

Yuce, O., Piekny, A., and Glotzer, M. (2005). An ECT2-centralspindlin complex regulates the localization and function of RhoA. J Cell Biol *170*, 571-582.

Zipkin, I. D., Kindt, R. M., and Kenyon, C. J. (1997). Role of a new Rho family member in cell migration and axon guidance in C. elegans. Cell *90*, 883-894.

Zipperlen, P., Fraser, A. G., Kamath, R. S., Martinez-Campos, M., and Ahringer, J. (2001). Roles for 147 embryonic lethal genes on C.elegans chromosome I identified by RNA interference and video microscopy. Embo J *20*, 3984-3992.

9. DECLARATION

I herewith declare that I have produced this paper without the prohibited assistance of third parties and without making use of aids other than those specified; notions taken over directly or indirectly from other sources have been identified as such. This paper has not previously been presented in identical or similar form to any other German or foreign examination board.

The thesis work was conducted from 01. September of 2001 to 02. September of 2005 under the supervision of Prof. Dr. Anthony Hyman at Max Planck Institute of Molecular Cell Biology and Genetics, Dresden, Germany.

Dresden, 02. Sepember 2005

Stephanie Schonegg